DYNAMIC TESTING OF A COMPOSITE MATERIAL HELICOPTER TRANSMISSION HOUSING

Roy A. Battles

Bell Helicopter Company

Prepared for:

Army Air Mobility Research and Development Laboratory

September 1975

USAAMRDL-TR -75-47

289089

DYNAMIC TESTING OF A COMPOSITE MATERIAL HELICOPTER TRANSMISSION HOUSING

Bell Helicopter Company
P. O. Box 482
Fort Worth, Tex. 76101

September 1975

Approved for public release; distribution unlimited.

Prepared for

EUSTIS DIRECTORATE
U. S. ARMY AIR MOBILITY RESEARCH AND DEVELOPMENT LABORATORY
Fort Eustis, Va. 23604

EUSTIS DIRECTORATE POSITION STATEMENT

The information contained in this report is the result of a program to test a graphite composite transmission housing fabricated under Contract DAAJ02-71-C-0059 by Whittaker Corporation, with Bell Helicopter Company as subcontractor.

The graphite composite housing was tested in a UH-1 bench test transmission. The spiral bevel gear development test indicated that the gear tooth pattern was improved by the stiffer housing. During preparation for the thermal mapping tests of the transmission, the adhesive bond in the input quill area failed. The damage was not repairable; therefore, the tests were terminated. A failure analysis was performed on the damaged graphite composite housing.

The report has been reviewed by the Eustis Directorate, U. S. Army Air Mobility Research and Development Laboratory and is considered to be technically sound.

The technical monitor for this program was Mr. Robert L. Rodgers, Technology Applications Division.

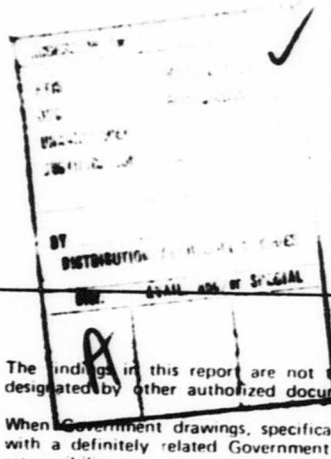

Unclassified

SECURITY CLASSIFICATION OF THIS PAGE (When Data Entered)

REPORT DOCUMENTATION PAGE

READ INSTRUCTIONS BEFORE COMPLETING FORM

1. REPORT NUMBER: USAAMRDL-TR-75-47
2. GOVT ACCESSION NO.
3. RECIPIENT'S CATALOG NUMBER

4. TITLE (and Subtitle): DYNAMIC TESTING OF A COMPOSITE MATERIAL HELICOPTER TRANSMISSION HOUSING

5. TYPE OF REPORT & PERIOD COVERED

6. PERFORMING ORG. REPORT NUMBER: 299-099-743

7. AUTHOR(s): Roy A. Battles

8. CONTRACT OR GRANT NUMBER(s): DAAJ02-73-C-0038

9. PERFORMING ORGANIZATION NAME AND ADDRESS:
Bell Helicopter Company
P. O. Box 482
Fort Worth, Texas 76101

10. PROGRAM ELEMENT, PROJECT, TASK AREA & WORK UNIT NUMBERS: 62208A 1F162208A170 03 010 EK

11. CONTROLLING OFFICE NAME AND ADDRESS:
Eustis Directorate, U. S. Army Air Mobility Research and Development Laboratory
Fort Eustis, Virginia 23604

12. REPORT DATE: September 1975

13. NUMBER OF PAGES: 79

14. MONITORING AGENCY NAME & ADDRESS(if different from Controlling Office)

15. SECURITY CLASS. (of this report): Unclassified

15a. DECLASSIFICATION/DOWNGRADING SCHEDULE

16. DISTRIBUTION STATEMENT (of this Report)

Approved for public release; distribution unlimited.

17. DISTRIBUTION STATEMENT (of the abstract entered in Block 20, if different from Report)

18. SUPPLEMENTARY NOTES

19. KEY WORDS (Continue on reverse side if necessary and identify by block number)

Composite materials
Composite structures
Expansion
Gears
Mapping
Thermal analysis

20. ABSTRACT (Continue on reverse side if necessary and identify by block number)

This program was carried out to investigate the integration of a GFE composite material gear housing into a UH-1 bench test transmission. The composite material housing was designed to replace a conventional magnesium sand cast housing. A test program using the composite housing was outlined to : (1) investigate tooling parameters and finish machine a housing; (2) determine the coefficients of ther-

DD FORM 1 JAN 73 1473 EDITION OF 1 NOV 65 IS OBSOLETE

Unclassified

SECURITY CLASSIFICATION OF THIS PAGE (When Data Entered)

mal expansion and thermal conductivity; (3) conduct a spiral bevel gear development test; (4) thermal map a transmission; (5) conduct a 50-hour overpower test; and (6) conduct a fail-safe test. The input quill area of the composite housing structurally failed while preparations were being made to thermal map a transmission. The remaining test program was cancelled, and failure analysis was performed on the composite housing.

Briefly, the test results are:

1. To prevent delamination, grinding had to be used almost entirely to machine the carbon-epoxy material.

2. The average coefficient of linear thermal expansion of the filament-wound carbon-epoxy liners in the housing bores in the circumferential direction was 2.0×10^{-6} in./in.-^{0}F for 123^{0}F to 350^{0}F. For comparison, the coefficient of linear thermal expansion of steel and magnesium is 6.3×10^{-6} in./in.-^{0}F and 14.0×10^{-6} in./in.-^{0}F, respectively.

3. The average thermal conductivity of the composite housing was .52 BTU/hr-ft-^{0}F for 141^{0}F to 203^{0}F. For comparison, the thermal conductivity of magnesium and asbestos is 92 BTU/hr-ft-^{0}F and .087 to .375 BTU/hr-ft-^{0}F, respectively.

4. The spiral bevel gear development test showed that the composite housing was slightly stiffer than a magnesium housing since the wear pattern on the input spiral bevel pinion teeth did not move as close to the heel as usual.

5. The failure analysis showed that the structural failure of the input quill area of the composite housing was the result of a defective main bearing ring-to-housing bond.

The structural failure of the composite housing showed that this particular design was not satisfactory for a helicopter transmission. However, the use of composite materials for helicopter transmission housings merits further investigation because of the potential of increased stiffness, strength, and tolerance to ballistic hits for the same or less weight.

PREFACE

This report contains the results of a test program for dynamic testing of a composite material helicopter transmission housing. The program was conducted by Bell Helicopter Company (BHC) for the Eustis Directorate, U.S. Army Air Mobility Research and Development Laboratory (USAAMRDL) from 8 March 1973 to 8 March 1975.

The program was performed under USAAMRDL Contract DAAJ02-73-C-0038.

USAAMRDL technical direction was provided by Robert L. Rodgers. The program was conducted under the technical direction of C. E. Braddock, Project Engineer, of the BHC Transmission Design Group. Acknowledgement for technical contribution is due H. Zinberg of the BHC Research Projects Group, who aided in the failure analysis.

TABLE OF CONTENTS

LIST OF ILLUSTRATIONS

LIST OF ILLUSTRATIONS (CONT'D)

LIST OF ILLUSTRATIONS (CONT'D)

LIST OF ILLUSTRATIONS (CONT'D)

LIST OF TABLES

INTRODUCTION

For many years, helicopter transmission housings have been made from aluminum or magnesium castings. These housings have good strength, stiffness, and thermal conductivity properties at a reasonable cost and weight. However, cast housings have very low tolerance to ballistic hits.

Advanced composite materials have been used successfully for numerous aircraft structures, such as drive-shaft tubes, control bellcranks, and airframe components. Most of these structures have been relatively simple from the standpoint of fabrication, machining, and number of load paths. The use of advanced composite materials for helicopter transmission housings offers the potential of improved stiffness, strength, and ballistic-hit tolerance for the same or less weight. In such an application, however, many formidable problems present themselves: multipath loading, development of machining techniques, heat transfer requirements, and installation of steel liners. The purpose of this program is to address these problems.

The composite transmission housing to be evaluated under this program was designed to replace an existing 204-040-353-23 magnesium housing used in the UH-1 transmission. The composite housing is shown in Figures 1 and 2, and the magnesium housing is shown in Figures 3 and 4. As shown in Figure 5, the housing is attached via bolted flanges to the ring gear housing above and a support housing below. The support housing is attached to the airframe by four elastomeric mounts and a lift link. This arrangement results in the -353-23 housing being subjected to torsional and lift loads during flight.

An additional function of the housing is to house and support the input spiral bevel pinion and gear and two accessory gears driven by the input spiral bevel gear. The input pinion loads are transferred to the housing via a triplex ball bearing located near the outer proximity of the housing and by a roller bearing located on the nose of the pinion. The input gear loads are transferred to the -353-23 housing via a duplex ball bearing mounted in a steering wheel housing which attaches to the top of the -353-23 housing and by a roller bearing located near the bottom of the -353-23 housing. Both forward and port bores are provided in the -353-23 housing to mount accessory drives.

The work outlined under the initial test program was to: (1) investigate tooling parameters and finish machine a housing; (2) determine the coefficients of thermal expansion and thermal conductivity; (3) conduct a spiral bevel gear development test; (4) thermal map a transmission; (5) conduct a 50-hour overpower test; and (6) conduct a fail-safe test.

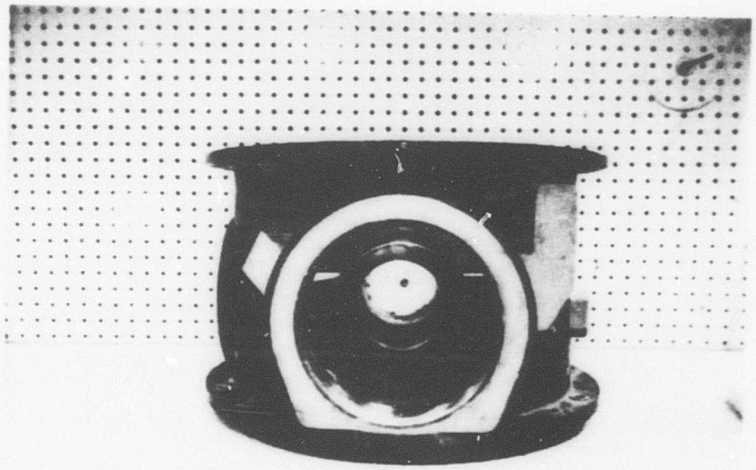

Figure 1. Input Quill Area of the Composite Housing.

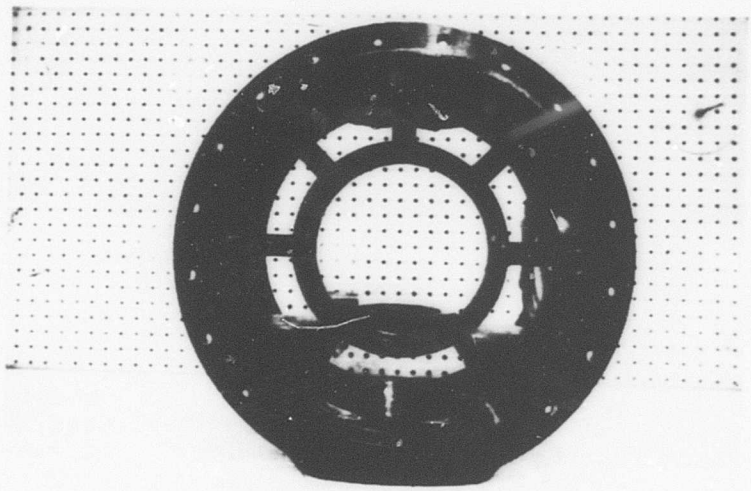

Figure 2. Bottom View of the Composite Housing.

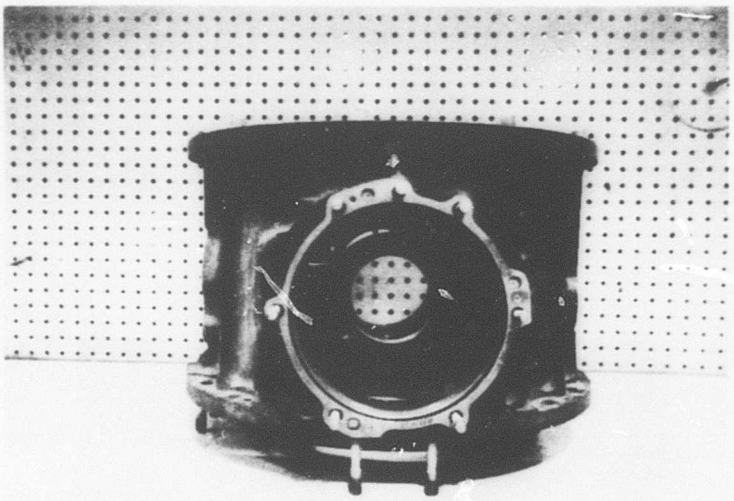

Figure 3. Input Quill Area of 204-040-353-23 Magnesium Housing.

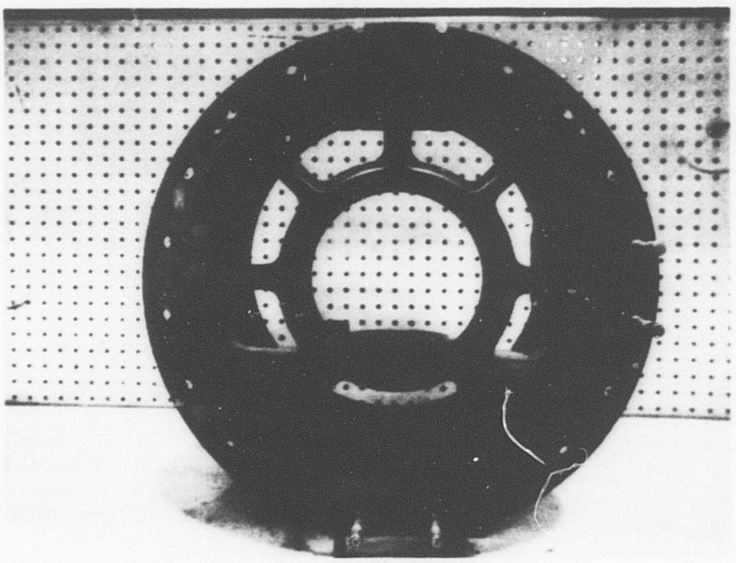

Figure 4. Bottom View of 204-040-353-23 Magnesium Housing.

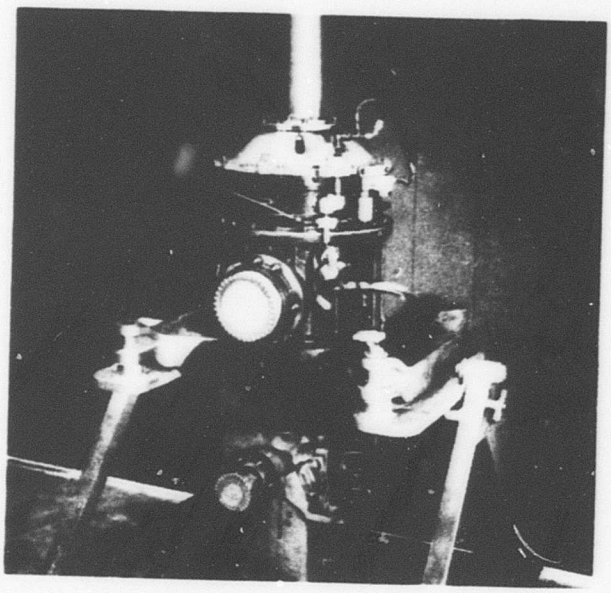

Figure 5. UH-1 Transmission Assembly.

Two composite housings were furnished by USAAMRDL to BHC for performing the test program. Serial Number (S/N) 1 housing was to be used to investigate machining and tooling requirements and to conduct the thermal expansion and conductivity analysis. S/N 2 housing was to be finish machined and assembled in a bench test transmission. A dimensional layout performed on S/N 2 housing revealed several discrepancies precluding the machining of the housing to a 204-040-353-23 blueprint configuration. The housing was returned to its manufacturer for rework. Subsequently, the discrepancies were corrected, the housing machined, and a bench test transmission assembled.

While preparations were being made to perform the spiral bevel gear development test, excessive leakage of oil through bond voids and cracks around the input quill bore was discovered. The housing was removed from the transmission, and the cracks and voids were sealed with a fluorinated silicone adhesive. After the transmission was reassembled, the spiral bevel gear development test was successfully completed.

The composite housing was instrumented and assembled in an instrumented transmission to perform a thermal map similar to the one performed under USAAMRDL Contract DAAJ02-72-C-0081.[1] During a shakedown run prior to the thermal map, the input quill area of the composite housing structurally failed. The remaining test program was cancelled, and a failure analysis was performed on the composite housing.

[1]Drennan, J. H., and Walker, R. D., TRANSMISSION THERMAL MAPPING (UH-1 MAIN ROTOR TRANSMISSION), USAAMRDL Technical Report 73-90, Eustis Directorate, U. S. Army Air Mobility Research and Development Laboratory, Fort Eustis, Virginia, December 1973, AD 777803.

TECHNICAL DISCUSSION

MACHINE TOOL INVESTIGATION

The composite transmission housing to be evaluated in this program is a complex structure due to cutouts for gear quills, lubricant fittings and passages, internal bearing mountings, and interfaces with housings above and below. Due to its complex nature, the housing requires extensive close-tolerance machining. Examples of some of the tolerances from the 204-040-353 blueprint (dimensions in inches) are 6.75025 ± .00025 input bore diameter; 5.0005 ± .0005 port and forward accessory bore diameters; 14.525 ± .002 0-ring diameter; 10.1555 ± .0025 top flange surface; .3125 ± .0005 oil jet hole; .37605 ± .00025 dowel pin holes; and a 63 AA finish on all machined surfaces.

As detailed in Reference 2, the material used for the housing was Narmco's 5208 prepreg, which is based on a high-temperature resin system and Modmor I carbon fibers. U. S. Polymeric's EM 7302 glass-epoxy bulk molding compound (BMC) was used for the bearing ring inserts and bosses. Components of the housing were bonded together with Hysol Dexter's EA-934 epoxy adhesive.

Since machining of composite materials is still in its infancy, S/N 1 composite housing was used to investigate tooling parameters and tooling requirements. Boring, drilling, and milling tests were conducted on the BMC and the carbon-epoxy materials of the housing.

No difficulties were encountered in machining the BMC material. The BMC material could be machined with the same tools and similar speeds and feeds as used on the production 204-040-353-23 magnesium housing.

Results of the boring test on the carbon-epoxy material are shown in Table 1. None of the methods in Table 1 yielded satisfactory results. To maintain size and to prevent delamination of the carbon-epoxy material, grinding was the only acceptable method found to machine the housing bores.

Results of the drilling test on the carbon-epoxy material are shown in Table 2. The fourth drilling configuration in Table 2 yielded satisfactory results.

Results of a milling test on the carbon-epoxy material are shown in Table 3. To maintain size and prevent delamination, grinding again was the only acceptable method found to machine the flat surfaces of the housing.

---

[2]Chase, V. A., INVESTIGATION OF THE USE OF CARBON COMPOSITE MATERIALS FOR HELICOPTER TRANSMISSION HOUSING APPLICATIONS, USAAMRDL Technical Report 73-7, Eustis Directorate, U. S. Army Air Mobility Research and Development Laboratory, Fort Eustis, Virginia, July 1973, AD 771978.

TABLE 1. BORING TEST

Tool Configuration						
Material	Angle	RPM	Feed (In.)	Approximate Length of Cut (In.)	Material and Location	Results
High-Speed Latrobe Steel (Dynavan)	10^0 positive rake, 15^0 lead, and .010 radius	350	.002	13.65 dia. x 1.06 deep	Laminated carbon-epoxy at O-ring surface near top flange	Approx. 125 surface finish, delamination, and no cutter life
Carbide Inserts	5^0 positive rake, 45^0 lead, and .010 radius	200	.004	3.75 dia. x 1.2 deep	Filament-wound carbon-epoxy liner in input pinion roller bearing bore	Approx. 125 surface finish, delamination, and no cutter life
Carbide Inserts	5^0 positive rake and 0^0 lead	200	.004	3.75 dia. x 1.2 deep	Filament-wound carbon-epoxy liner in input pinion roller bearing bore	Approx. 63 surface finish, delamination, and no cutter life
Carbide Inserts	5^0 positive rake and 0^0 lead	420	.002	3.75 dia. x 1.2 deep	Filament-wound carbon-epoxy liner in input pinion roller bearing bore	Approx. 63 surface finish, slight delamination, and no cutter life

TABLE 2. DRILLING TEST*

Drill Configuration						
Size (In.)	Material	Point	RPM	Feed (In.)	Depth (In.)	Results
3/8	High-speed steel	118° angle, non-split	125	.002	1/8	Delamination
3/8	High-speed steel	118° angle non-split	250	.003	1/8	Hole tolerance not maintained and delaminated
3/8	High-speed steel	135° angle, split	125	.002	1/8	Approx. 125 surface finish and delamination
3/8	Carbide	135° angle, non-split	1500	.002	1/8	Approx. 63 surface finish, hole tolerance maintained, and no delamination

*Test performed on laminated carbon-epoxy lower flange.

TABLE 3. MILLING TEST*

Cutter Configuration							
Size (In.)	No. of Flutes and Material	Angle	RPM	Feed (In.)	Approximate Length of Cut (In.)	Chip Load (In.)	Results
1.25 Dia.	2 flute carbide insert	0° rake, .030 radius, and 5° - 12° primary relief	1100	20	18	.010	Bad surface finish (>125) and delamination

*Test performed on face of input quill bore. Cut passed through BMC, filament-wound carbon-epoxy, and laminated carbon-epoxy.

CASE MACHINING AND ASSEMBLY

While S/N 1 housing was being used to investigate machining and tooling requirements, a dimensional layout was performed on S/N 2 housing. The dimensional layout revealed several discrepancies, precluding a finish machined housing to the 204-040-353-23 blueprint configuration. The S/N 2 housing was returned to its manufacturer to be reworked.

The discrepancies and the method by which they were corrected are outlined below. All dimensions are in inches.

1. Ten .495 diameter thru holes and two tapped holes were already in the bottom flange (Surface "T") upon receipt of the housing. The blueprint requires twelve .390/.396 diameter thru holes located with respect to the centerline of the finish machined input pinion bore. The discrepancy was corrected by bonding solid steel inserts in the holes.

2. Six 3/8-16UNC-3B tapped holes were already in the bottom flange (Surface "T") upon receipt of the housing. The blueprint required the tapped holes to be located with respect to the centerline of the finish machined input pinion bore. The discrepancy was corrected by filling the holes with bulk molding compound (BMC).

3. The dimension from the centerline of the input pinion bore (Diameter "J") to the lower surface of the bottom flange (Surface "T") would machine to approximately 4.110 to cleanup. The blueprint required the dimension to be 4.122/4.127. The required machining stock was provided by laying on additional carbon-epoxy material to Surface "T".

4. Twenty .495 diameter thru holes were already in the top flange (Surface "U") upon receipt of the housing. The blueprint required twenty .390/.396 diameter thru holes located with respect to the centerline of the finish machined input pinion bore. The discrepancy was corrected by bonding solid steel inserts in the holes.

5. There was not enough machine stock for the .938 diameter counterbore located near the bottom of the input pinion bore. The counterbore houses the oil transfer tube. The required machining stock was provided by laying on additional BMC material.

6. The O-ring sealing diameter (Diameter "S") located near the top flange would machine to approximately 14.250 to cleanup. The blueprint required Diameter "S" to be 13.750/13.752. Additional carbon-epoxy material was laid onto Diameter "S" by the housing manufacturer. However, after the housing was returned to BHC, it was necessary to provide additional machining stock by building up the areas still lacking in material with Ren Plastic, Inc. RP-1220, a two-part epoxy. BHC has used the RP-1220 epoxy to make similar repairs on bench test housings in the past.

7. The input bore (Diameter "J") to the port accessory bore (Diameter "M") and the input bore (Diameter "J") to the forward accessory bore (Diameter "AL") were not 90 degrees and 180 degrees, respectively positioned. Due to the extensive rework that would have been required, no correction was attempted. The bores were machined per blueprint, resulting in portions of the filament-wound carbon-epoxy liners in the left and forward accessory bores being machined away. This discrepancy did not affect the bench test program since dummy quills (quills without gears) were used in both accessory bores.

8. The oil jet pad (number 6) located on the right side of the housing was mislocated down .182 and forward .200. The oil jet pad houses the input pinion roller bearing oil jet. The discrepancy was corrected by laying on additional BMC material.

9. The boss that houses the input pinion roller bearing oil jet inside the housing was omitted. The boss is located to the right side of the bore for the input pinion roller bearing. The discrepancy was corrected by molding a boss of BMC material and bonding it onto the housing.

10. The oil manifold pad located to the right side of the input bore was mislocated .121 toward the input bore. The discrepancy was corrected by laying on additional BMC material.

11. The oil jet pad (number 5) located to the left side of the input bore was mislocated up 1.000. The pad houses the oil jet for the input pinion/gear mesh. The discrepancy was corrected by laying on additional BMC material.

After the housing was returned to BHC, four additional discrepancies were discovered during machining. The first of the

four discrepancies is discussed in item 6 above, and the remaining three are discussed below.

12. The boss inside the housing that houses the oil jet (number 5) for the input pinion/gear mesh had been omitted. The boss is located to the left side of the input bore. Repairs to the housing were made by thermal fitting a steel sleeve in the housing to house the oil jet. The sleeve was also pinned in place to insure that it did not rotate during bench test. BHC has used similar repairs in the past on transmission housings.

13. The bolt holes required by the blueprint to pass through the lower flange on either side of the input bore were not machined in the housing. The holes are spot faced on the upper surface of the bottom flange. A large portion of the composite housing would have been machined away to spot face the required area, which could have seriously weakened the input quill area of the housing. The composite housing has more material in this area than a production magnesium housing. Omission of the two studs was not detrimental to the bench test program since the housing was not subjected to flight lift loads.

14. Two of the 12 bolt holes drilled in the steel inserts of the bottom flange and 14 of the 20 bolt holes drilled in the steel inserts of the top flange were partially in the carbon-epoxy material. The discrepancy resulted from the mispositioning of the steel inserts with respect to the centerline of the input pinion bore. No attempt was made to correct the discrepancy since the structural integrity or the functional requirements of the housing were not affected.

The composite housing was successfully machined to 204-040-353-23 blueprint configuration except for the discrepancies listed above. The composite housing required 174 manufacturing man-hours to machine. Approximately 17 manufacturing man-hours are required to machine the production magnesium housing. The man-hours required to machine the respective housings are included for information only and should not be used for comparison. In a high-production environment, the man-hours required to machine the composite housing would diminish and could conceivably approach the man-hours required to machine the magnesium housing.

The final operation required to ready the housing for assembly in a bench test transmission was the installation of studs,

inserts and lock rings, washer seats, and shims. The installation of the studs in the housing required .003- to .012-inch oversize studs to meet the blueprint torque requirements. The stud installation also revealed that the same stud reinstalled in the hole from which it was removed required only approximately 50 percent of the original installation torque. Installation of the washer seats caused small surface cracks in the BMC. The remaining items were installed without incident.

THERMAL EXPANSION ANALYSIS

The objective of this test was to determine the coefficient of thermal expansion from 100°F to 350°F in 50-degree increments for the bearing liner bores and the gear quill bores. From this data, the correct interference fit for the liners was calculated.

The coefficient of thermal expansion was determined by comparing the output of strain gages bonded to the S/N 1 housing and those bonded to a known calibration material. This comparison can be expressed mathematically as

$$\alpha_H = (2.4 \times 10^{-6} \text{ in./in. } -^0\text{F}) \Delta L_H / \Delta L_t$$

Tungsten was selected as a calibration material because of its almost constant coefficient of thermal expansion over a broad temperature range. Per Reference 3, the coefficient of thermal expansion for tungsten is 2.4×10^{-6} in./in. $-^0$F. The equipment required for the test included strain gages, a recording oscillograph, a temperature recorder, and an oven in which to heat the housing and tungsten bar. The test setup is shown in Figures 6 and 7.

Both large and small size strain gages of the same type were available for the test. In order to select the gage size best suited for the test, a preliminary test was conducted with one gage of each size bonded in the input quill bore. Between the temperatures of 250°F and 300°F, the large size gage indicated zero strain. Examination of the input quill bore revealed the gage had failed because it had been placed over a hairline crack in the circumferentially wound graphite liner. The smaller size gages were selected since they could be positioned to avoid cracks in the housing bores.

After completion of the gage evaluation test, all of the bores in the S/N 1 and S/N 2 housings were dye-penetrant inspected. As shown in Figures 8 through 11, all of the bores in the S/N 1 housing had hairline cracks except the one for the input pinion roller bearing. All of the bores in the S/N 2 housing, including the input pinion roller bearing bore, were similarly

[3]Weber, R. L., White, M. W., and Manning, K. V., COLLEGE PHYSICS, 3rd Edition, New York, McGraw-Hill Book Company, 1959.

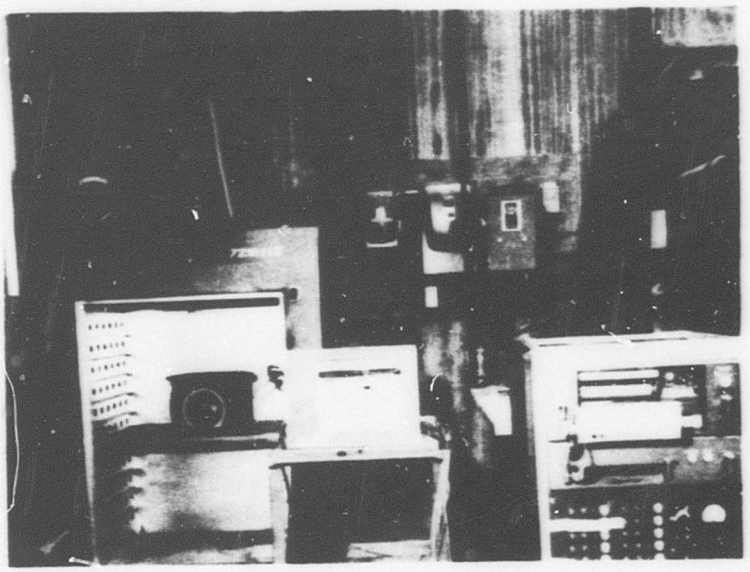

Figure 6. Test Setup for Thermal Expansion Analysis.

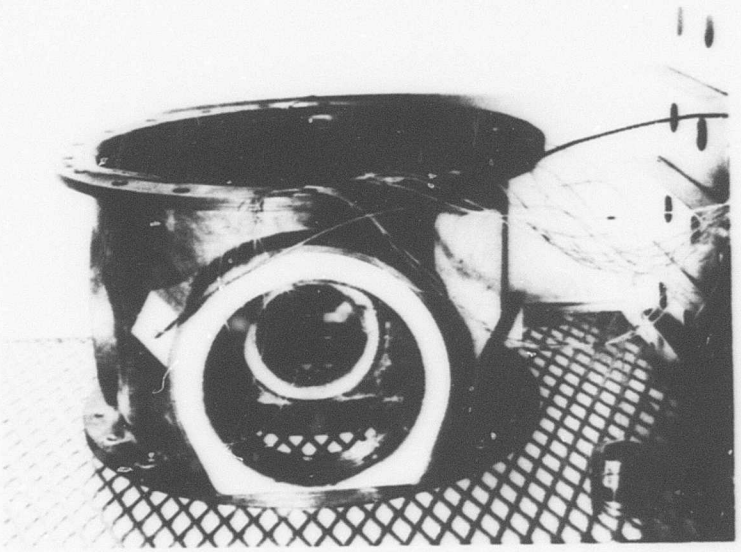

Figure 7. Instrumented Housing and Tungsten Bar in Oven.

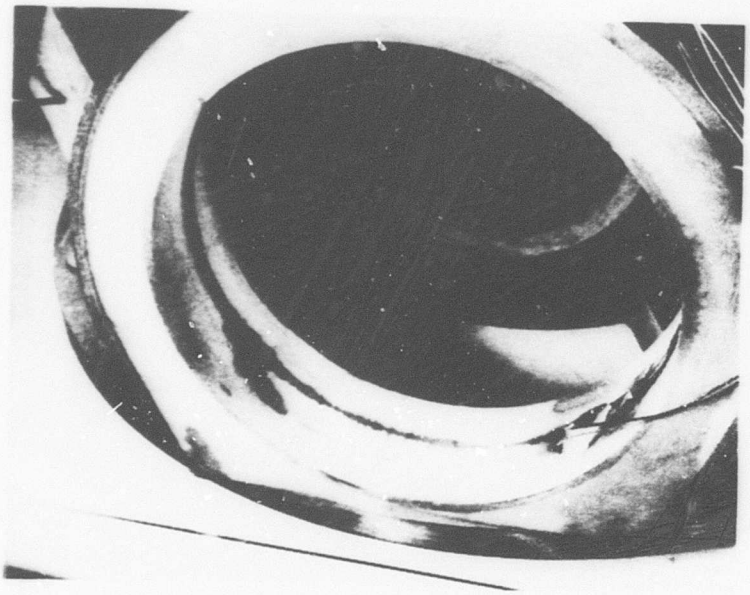

Figure 8. Crack in the Input Quill Bore of S/N 1 Housing.

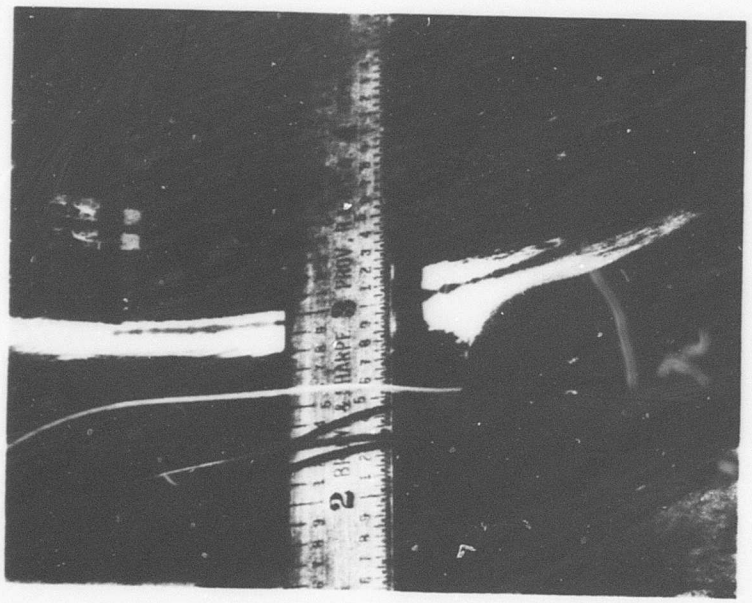

Figure 9. Close-up of Crack in the Input Quill Bore of S/N 1 Housing.

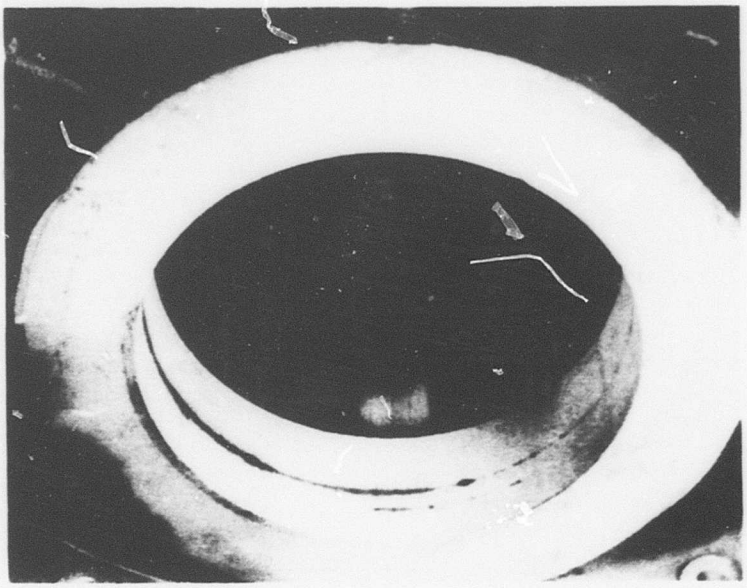

Figure 10. Crack in the Left-Side Accessory Bore of S/N 1 Housing.

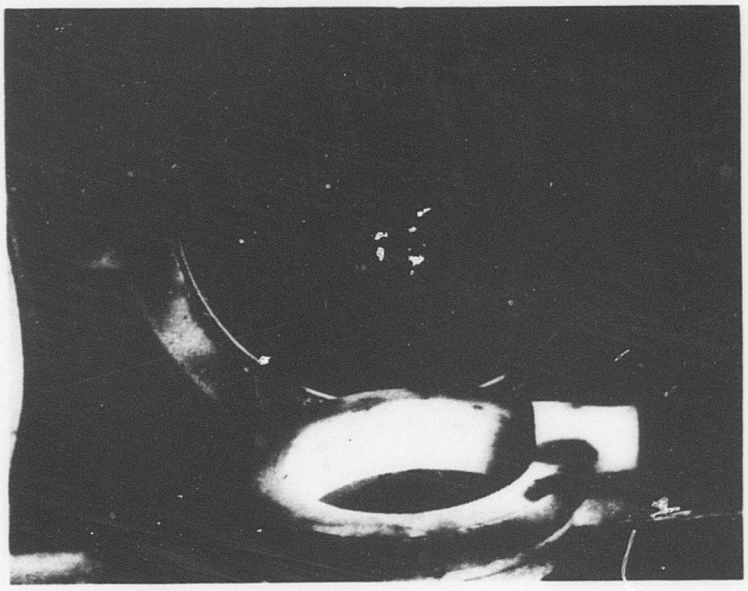

Figure 11. No Cracks in the Input Pinion Roller Bearing Bore of S/N 1 Housing.

cracked. The cracks in the input and accessory quill bores were located approximately in the same plane as the intersection of the housing cylindrical wall and the quill bores. It is possible that a thermal expansion differential between the housing wall and the quill bores could have caused the graphite liners to crack. As shown in Figures 12 and 13, the graphite liner in the bore for the input gear roller bearing was severely cracked. These cracks could possibly have been caused by a thermal expansion differential between the graphite liner and the surrounding nine webs.

Two strain gages in a circumferential direction and one in the axial direction were bonded in each bore except the input gear roller bearing bore. Only one gage in the circumferential direction could be bonded in the input gear roller bearing bore due to the numerous cracks.

The output from the gages positioned in the axial direction exceeded the recording oscillograph scale on the initial test. The recording oscillograph scale factor was readjusted, and the test was repeated with more satisfactory results. The results of Tests 1 and 2 are plotted in Figures 14 and 15, respectively. From the test results, the average coefficient of linear thermal expansion in the circumferential direction was calculated to be 2.0×10^{-6} in./in.-^{0}F for 123^{0}F to 350^{0}F. The coefficient of linear thermal expansion in the axial direction varied from 8.2×10^{-6} in./in.-^{0}F at 130^{0}F to 16.9 in./in.-^{0}F at 250^{0}F. Due to this wide variation, it was not feasible to calculate an average coefficient of linear thermal expansion in the axial direction.

Using the average coefficient of linear thermal expansion in the circumferential direction, the interference fit for the input pinion and gear roller bearing liners was calculated. A line-to-line fit at -40^{0}F was selected as the basis for the liner fit. The thermal expansion calculations and interference fit calculations are shown in Appendix A.

THERMAL CONDUCTIVITY ANALYSIS

The objective of this test was to determine the thermal conductivity of the composite housing. The thermal conductivity of the composite housing differing significantly from the thermal conductivity of the production magnesium housing would affect the transmission cooling system and the operating environment of the bearings and gears mounted in the composite housing.

The thermal conductivity of the housing was determined by using a heat source inside the housing with all openings sealed with asbestos sheet. The temperature difference across the housing

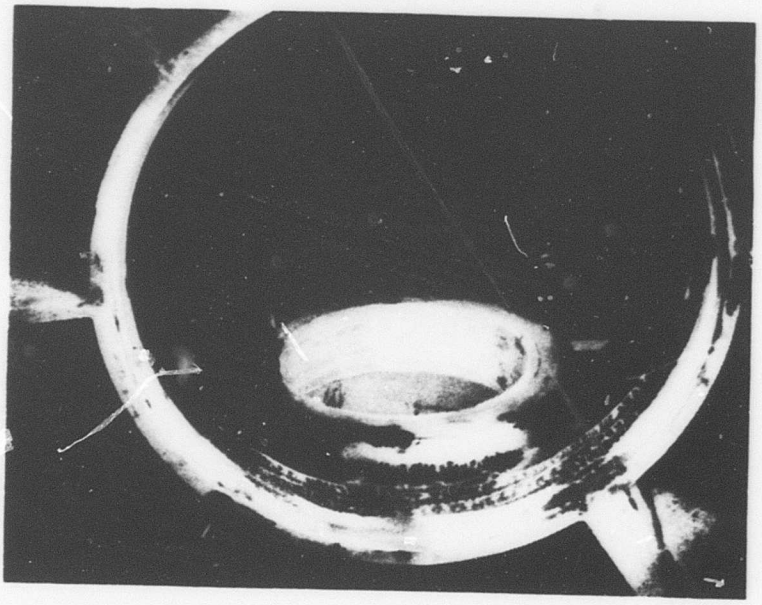

Figure 12. Cracks in the Input Gear Roller Bearing Bore of S/N 1 Housing.

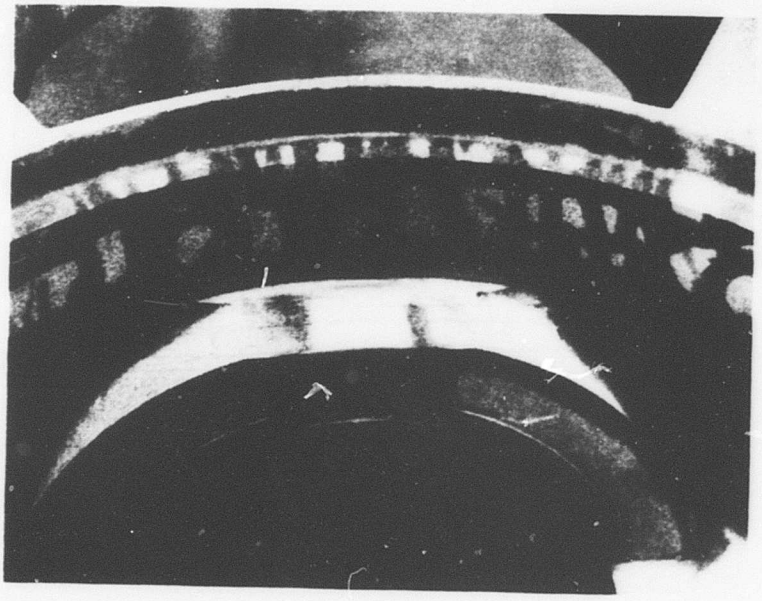

Figure 13. Cracks in the Input Gear Roller Bearing Bore of S/N 2 Housing.

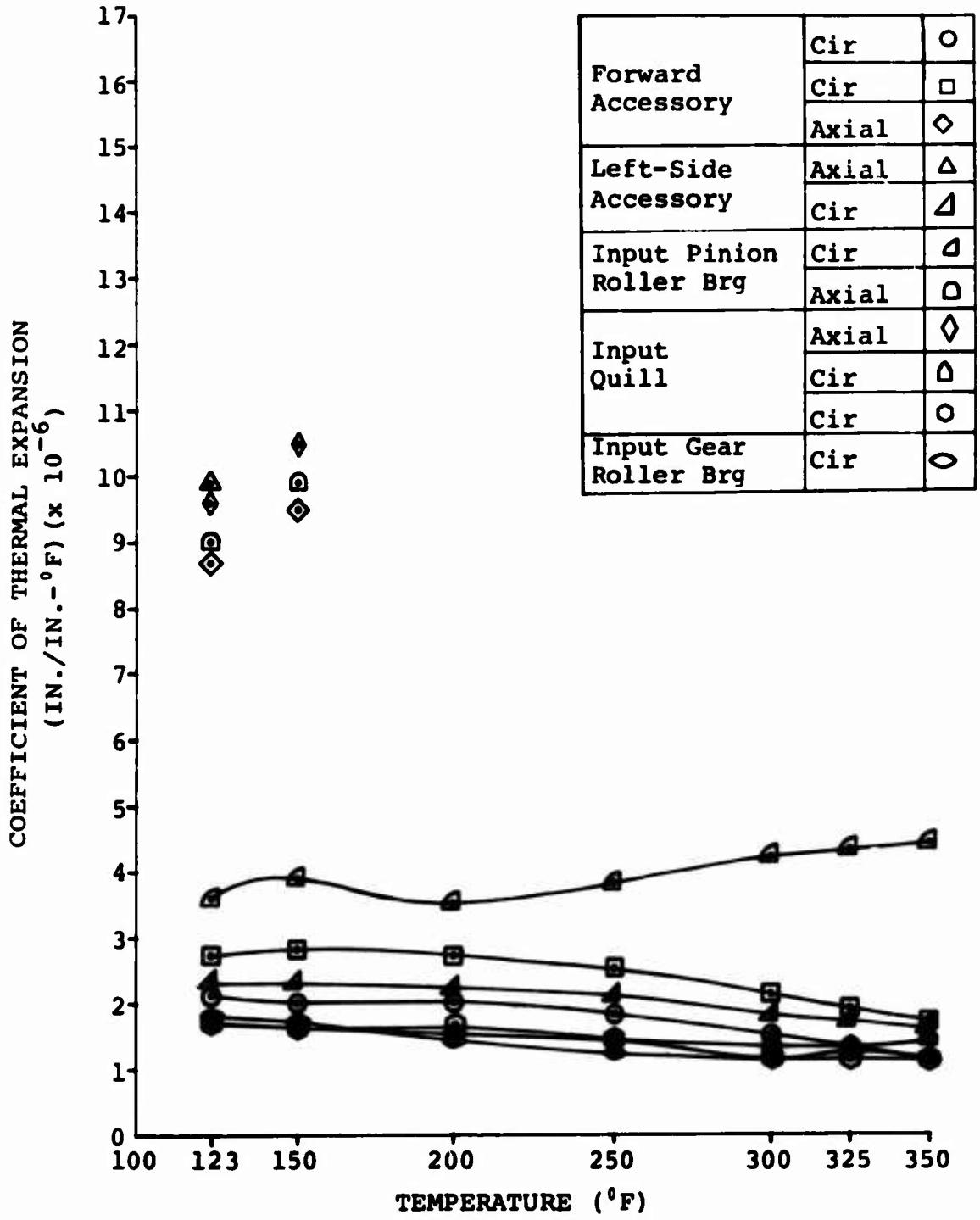

Figure 14. Coefficient of Thermal Expansion, Test 1

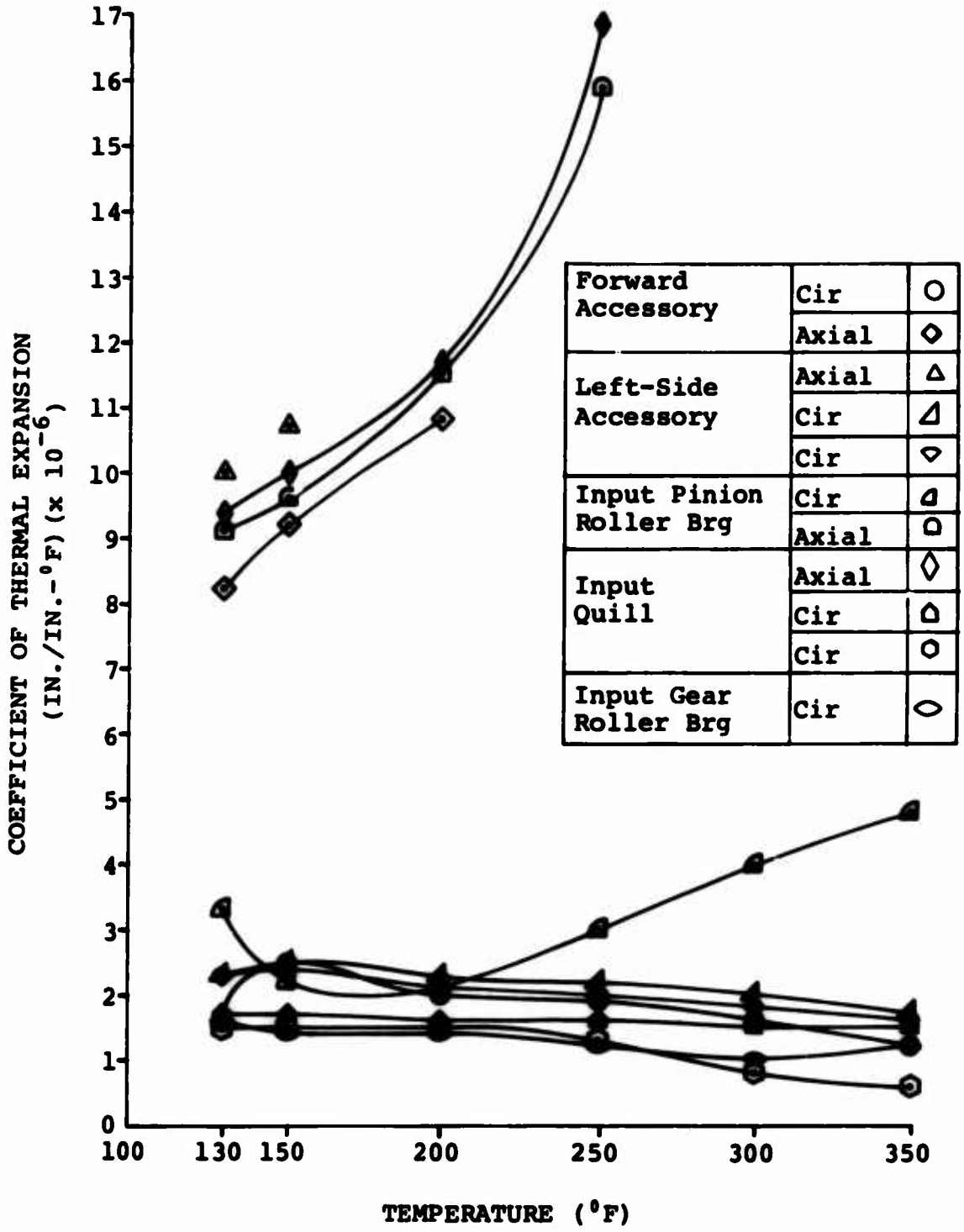

Figure 15. Coefficient of Thermal Expansion, Test 2

wall and asbestos sheet was measured by special temperature-sensitive strain gages. By knowing the amount of heat put into the housing, the thermal conductivity of the asbestos sheet, and the temperature differences across the housing wall and asbestos sheet, the thermal conductivity of the housing was calculated.

Equipment required for the test included nickel foil temperature strain gages, a recording oscillograph, a temperature recorder, a potentiometer calibration device, an oven, 1-inch-thick asbestos sheet, and a 1500-watt heating element with manually operated thermostat. The test setup is shown in Figure 16.

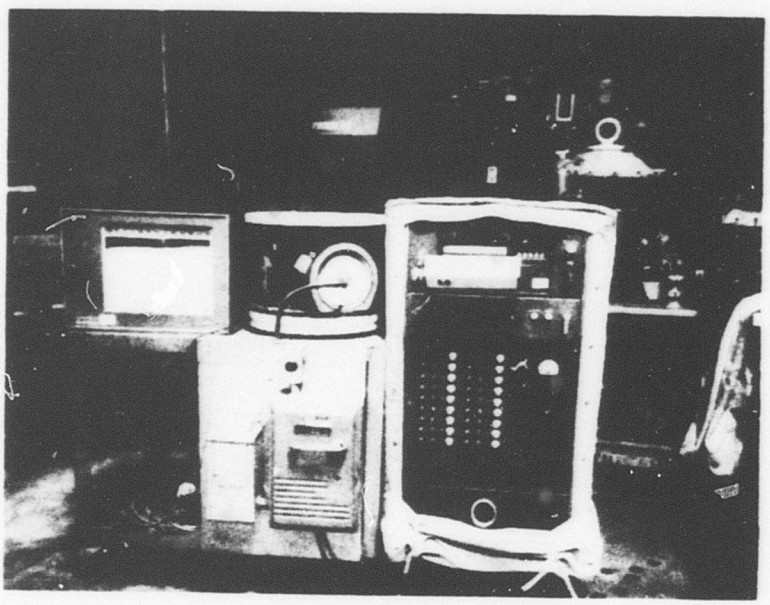

Figure 16. Test Setup for Thermal Conductivity Analysis.

The heating element was located inside the case, and all openings were sealed with the asbestos sheet as shown in Figures 17 and 18. The strain gages were located as shown in Figure 19. Locating the gages in pairs directly opposite each other and using a matching network, the oscillograph deflection represented the temperature difference across the wall. After the output of the strain was calibrated as detailed in Appendix B, the temperature difference across the wall at the

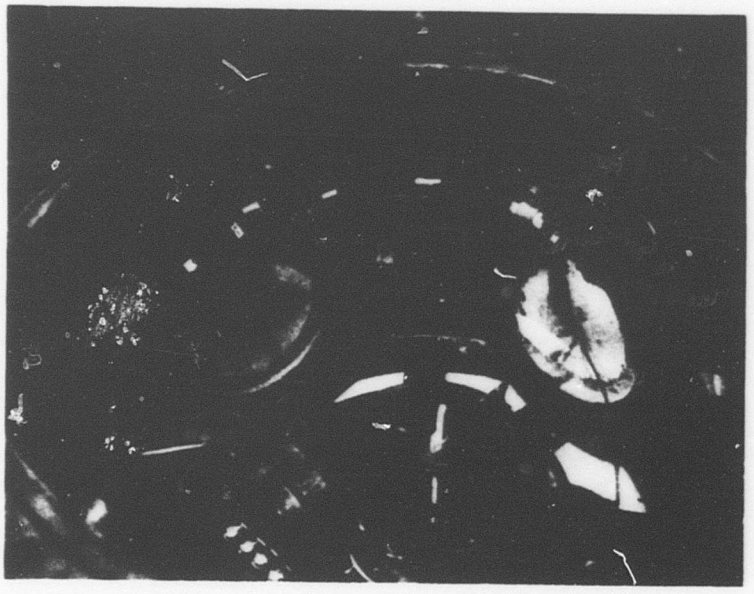

Figure 17. Housing Internal Test Setup for Thermal Conductivity Analysis.

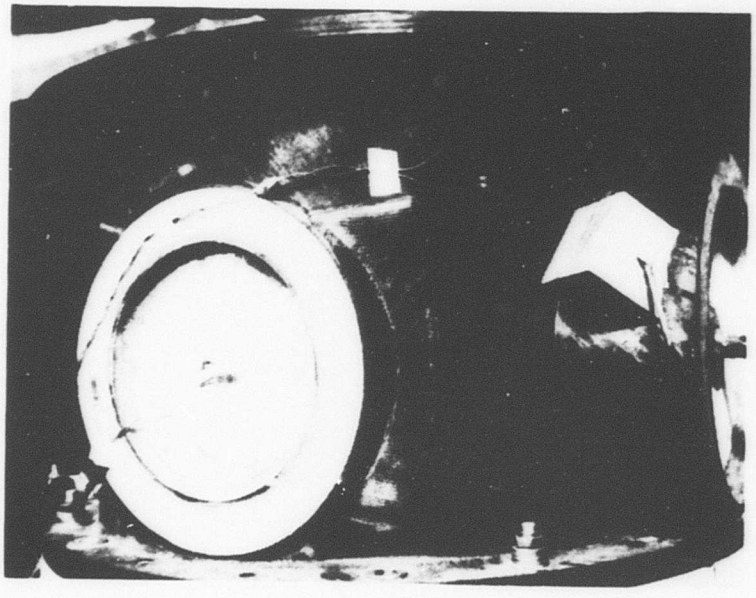

Figure 18. Housing External Test Setup for Thermal Conductivity Analysis.

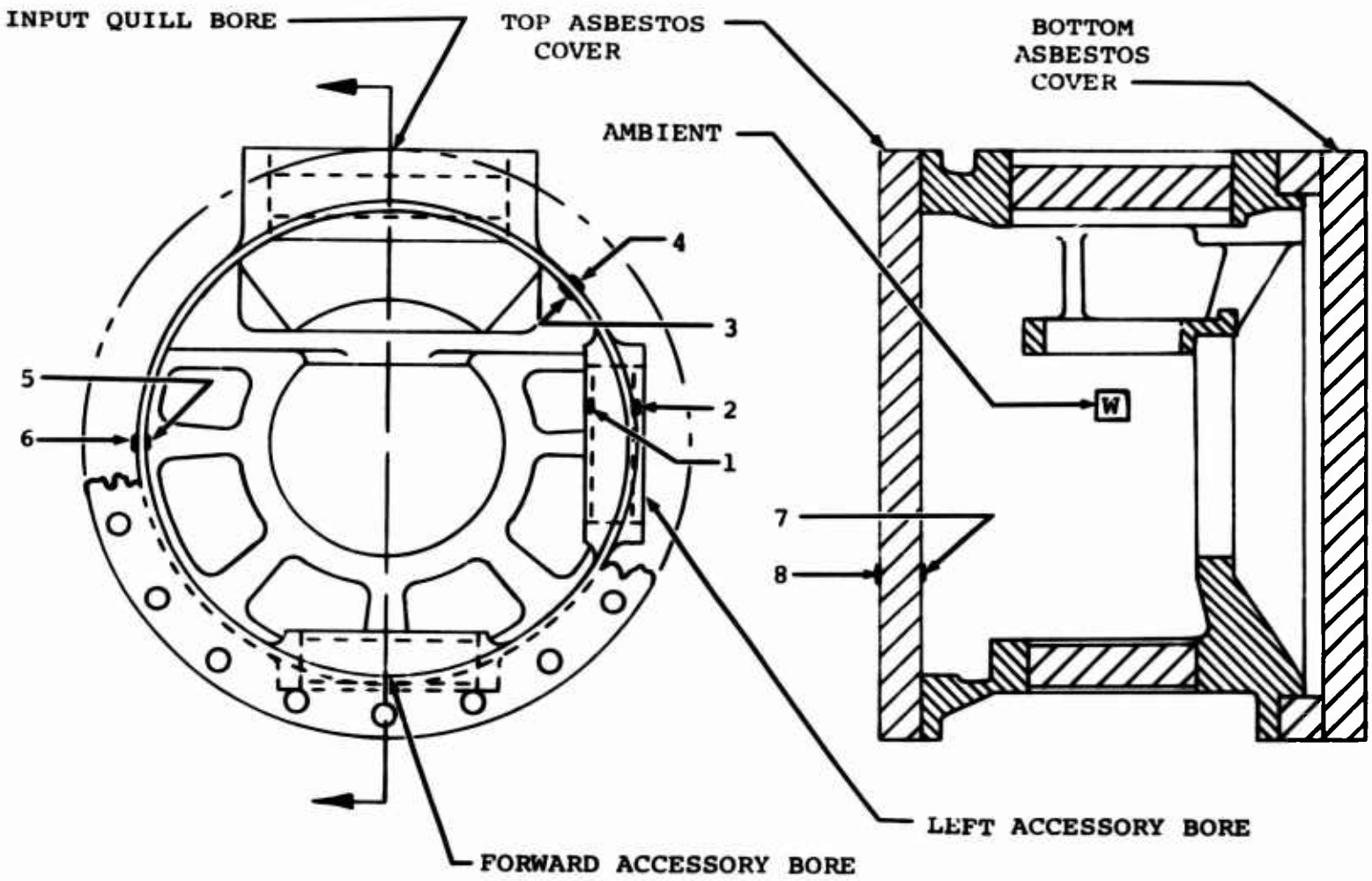

Figure 19. Location of Temperature-Sensing Strain Gages.

four locations was measured at three internal steady-state temperatures: 203°F, 193°F, and 141°F. The thermal conductivity of the housing at each temperature was calculated as shown in Appendix C.

The average thermal conductivity of the housing was calculated to be .52 BTU/hr-ft-°F. The very low thermal conductivity of the carbon-epoxy material would classify it as a very good insulator which is not desirable for a transmission housing material. For comparison, the thermal conductivity of magnesium and asbestos[4] is 92 BTU/hr-ft-°F and .087 to .375 BTU/hr-ft-°F, respectively. Future use of similarly configured composite transmission housings would require an increase in the capacity of the transmission cooling system since the carbon-epoxy material conducts .6 percent as much heat as magnesium.

The effect of the low thermal conductivity of the composite housing on the transmission cooling system was scheduled to be determined during the thermal map test. However, due to the structural failure of the input quill area of the housing, the thermal map test could not be performed.

SPIRAL BEVEL GEAR DEVELOPMENT TEST

To distribute the load on the teeth, aircraft spiral bevel gears are developed to operate in a particular gearbox. Development is required since each gearbox design has its own deflection characteristics. The development involves the operation of the spiral bevel gear set in the gearbox, the inspection of the tooth wear patterns to determine load distribution, and, if necessary, the regrinding of the pinion teeth. The development procedure may have to be repeated several times before an acceptable wear pattern is achieved.

Since it was possible that the mounting deflections for the input spiral bevel pinion and gear in the composite housing differed significantly from the deflections in the production 204-040-353-23 magnesium housing, a spiral bevel gear development test was conducted. Prior to assembling a test transmission, extensive gear tooth pattern checks for the input spiral bevel pinion and gear were made on a Gleason test machine. The purpose of the pattern checks was to insure that the gears were per blueprint and to aid in redevelopment of the pattern, if necessary.

A test transmission was assembled using the components from S/N A12-59 GFE transmission, the composite housing, an offset generator quill without gear in the forward accessory bore, and a side-mounted generator quill without gear in the left accessory bore. The dummy accessory quills were used so that

[4]Kreith, F., PRINCIPLES OF HEAT TRANSFER, 2nd Edition, Scranton, Pennsylvania, International Textbook Company, 1966.

the composite housing would have the same stiffness benefit as a magnesium housing during bench test.

The spiral bevel gear development test was to be conducted per the schedule shown in Table 4.

TABLE 4. LOAD SCHEDULE FOR SPIRAL BEVEL GEAR DEVELOPMENT TEST

Step	Step Time (Hr)	Percent Power	Input RPM	MAST OUTPUT Torque (In.-Lb)	HP
1	As Required	0-25	0-6600	0-53,659	0-275
2	1	25	6600	53,659	275
3	1	50	6600	107,318	550
4	1	75	6600	160,977	825
5	1	100	6600	214,636	1100
6	1	125	6600	268,295	1375

Operation during the initial step revealed excessive leakage of oil through bond voids and cracks around the input quill bore. The leaks were serious enough to prevent further use of the housing unless it could be sealed. USAAMRDL requested BHC to attempt to seal the housing so that the bench test program could be conducted.

The housing was twice sent through a vacuum impregnation process per Bell Process Specification (BPS) 4432. The vacuum impregnation process uses a thermosetting polyester resin of low viscosity designed specifically for impregnation of porous magnesium and aluminum transmission housings. The housing was then pressure tested as shown in Figure 20 without reassembling in a test transmission. The impregnation process had no appreciable effect on the oil leaks, and additional leaks were discovered inside the housing around the input quill bore. Figures 21 through 23 show the location of the leaks.

An additional problem, discovered during the pressure test, was the failure of the threads for the inserts in the oil manifold pad. The failure of the threads in the bulk molding

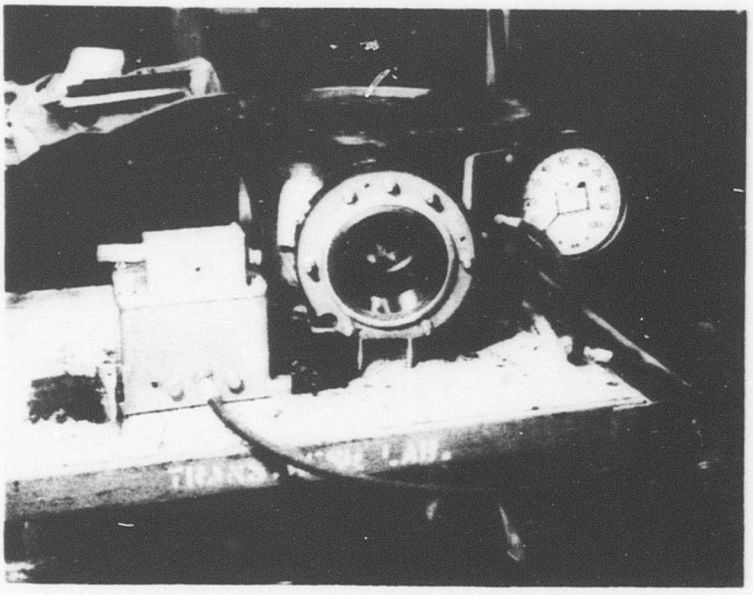

Figure 20. Pressure Test Setup After Vacuum Impregnation.

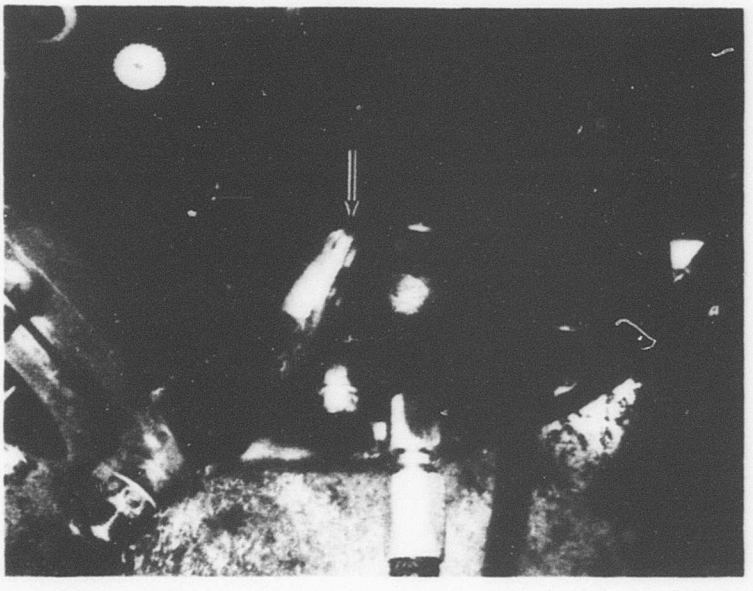

Figure 21. Oil Leak Adjacent to Oil Manifold Pad After Vacuum Impregnation.

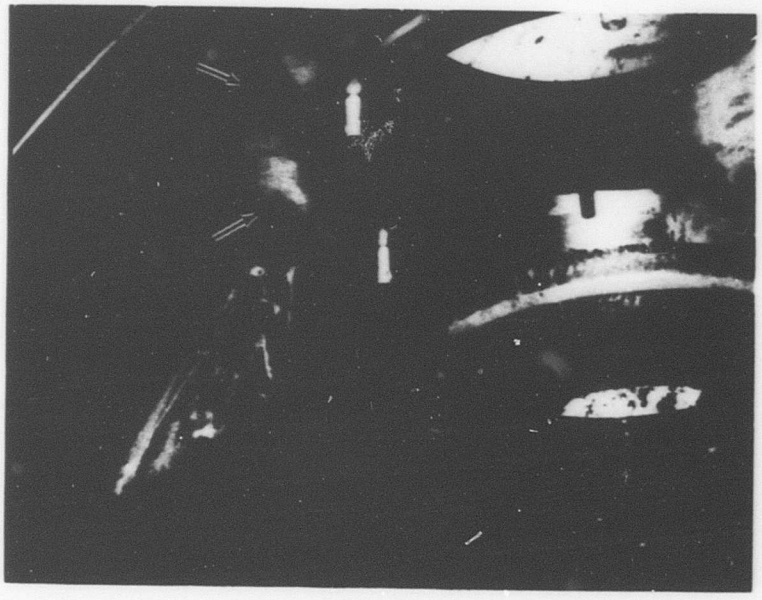

Figure 22. Oil Leak Coming From the Main Bearing Ring-to-Housing Bond After Vacuum Impregnation.

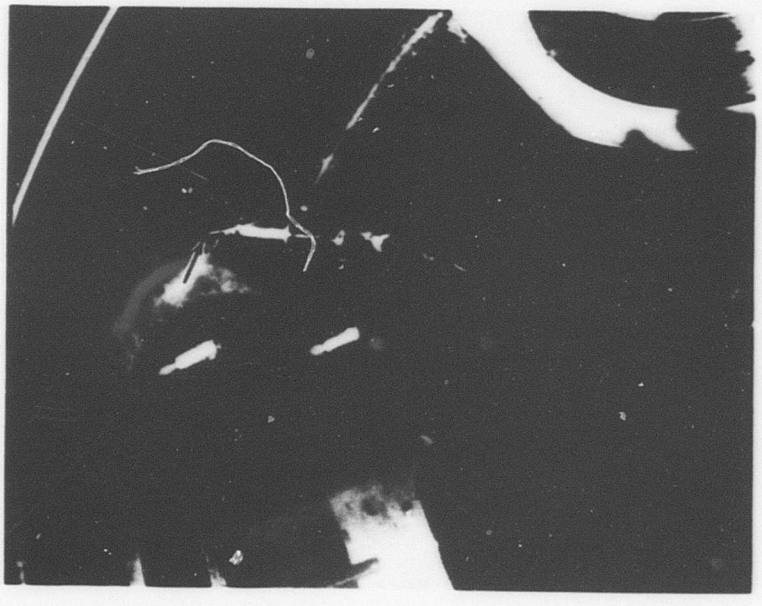

Figure 23. Oil Leak Near the Input Pinion/Gear Mesh Oil Jet After Vacuum Impregnation.

compound (BMC) was not unexpected since the BMC has only 49 and 25 percent of the shear strength of the magnesium housing at 70°F and 350°F, respectively. The failed threads were repaired by laying on Hysol Dexter EA-934, retapping, and installing inserts with 35 percent more shear area.

A second attempt at sealing the housing was successful. The oil passages entering and exiting the input bore were drilled oversize, and a sealant was injected through the passages. Pins were centered in the oversize oil passages prior to injecting the sealant. After the sealant had cured, removal of the pins left a cylinder of the sealant lining the oil passages. The sealant was injected into a vee (both inside and outside the housing) which was machined into the BMC at the main bearing ring-to-housing bond. The sealant used was Dow Corning RTV 20-046 fluorinated silicone, oil and fuel resistant, -65°F to 500°F temperature range. The BHC designation for the sealant is 299-947-152, Type III.

While the housing was being cleaned prior to the second sealing attempt, it was mistakenly immersed in the trichloroethylene of a vapor degreaser for 2 hours. Some visible damage to the housing occurred. As shown in Figures 24 and 25, flaking from the surface of the BMC occurred. Most of the flaking came from the BMC that was added to the housing by its manufacturer to correct deficiencies so that the housing could be machined to blueprint specification. The damage was minor, and no repairs to the BMC were necessary.

After the housing was sealed with the fluorinated silicone, it was pressure tested using 60-psi air and soapy water brushed onto the housing surface. The pressure test revealed that the housing still had some small leaks as shown in Figures 26 through 29. However, the leaks were not serious enough to prevent resumption of the spiral bevel gear development test.

After a test transmission of the configuration previously described was reassembled, the spiral bevel gear development test was successfully completed. The initial step of the schedule shown in Table 4 was used to check for proper lubrication distribution and scavenge and to check the function of the remaining system at low powers. After the completion of each step, the input pinion quill was removed from the housing and photographs of the wear patterns were made. Figures 30 through 34 show the drive side wear pattern on the input pinion after each step. Since the loads are approximately the same, the wear pattern after Step 5 can be compared to the acceptance test wear pattern from Reference 5, shown in Figure 35. The comparison reveals that the pattern is slightly low on the tooth, but acceptable, and that the composite housing is slightly

[5]Hopfensperger, L. J., SPECIFICATION FOR THE 204-040-009, 204-040-016, AND 205-040-001 TRANSMISSION ASSEMBLIES, BHC Report 204-947-153, Bell Helicopter Company, Fort Worth, Texas, February 1964.

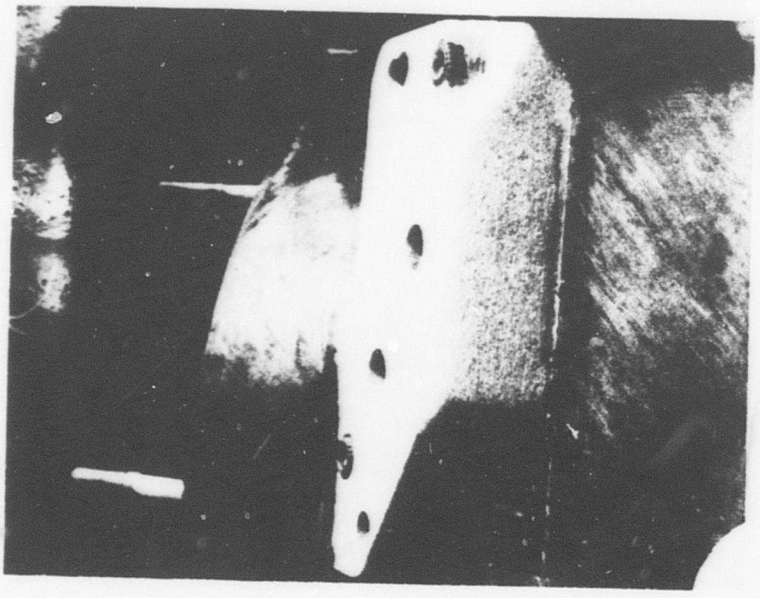

Figure 24. Flaking From BMC Oil Manifold Pad and Thread Failures.

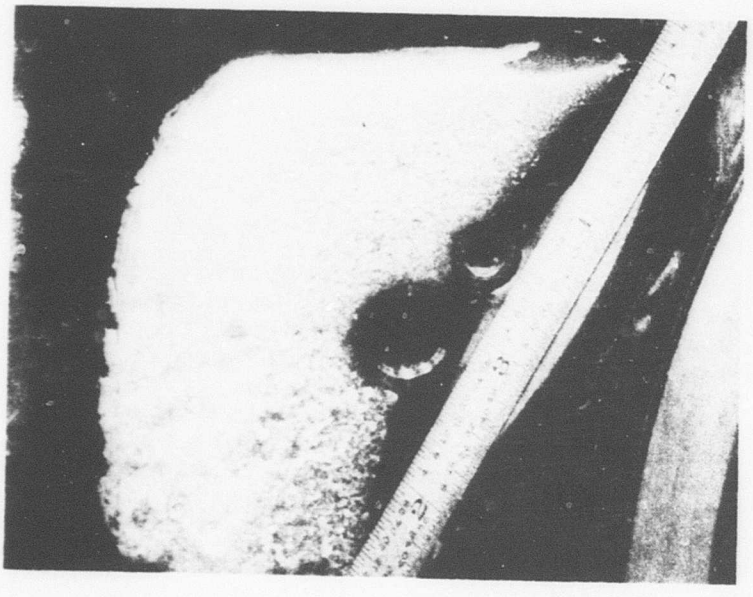

Figure 25. Flaking From BMC Oil Jet Pad for Input Pinion/Gear Mesh Oil Jet.

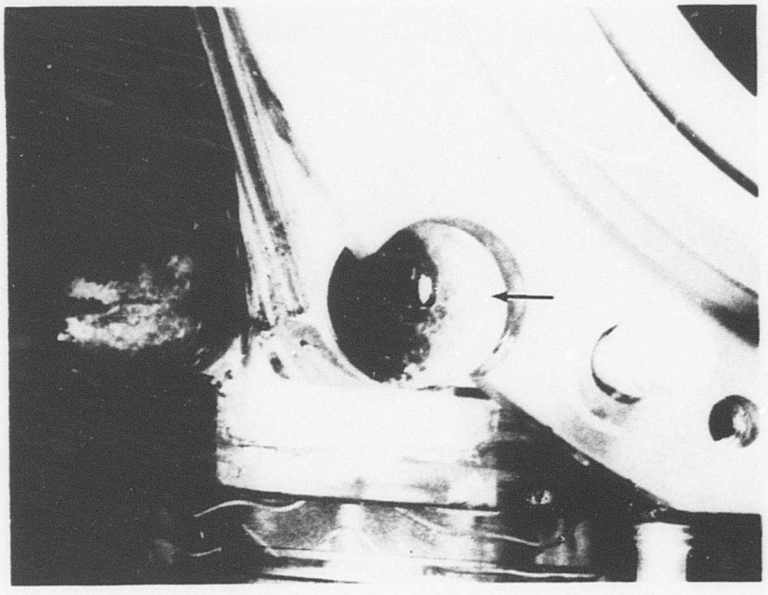

Figure 26. Leak in Oil Transfer Tube Bore After Sealing With Fluorinated Silicone.

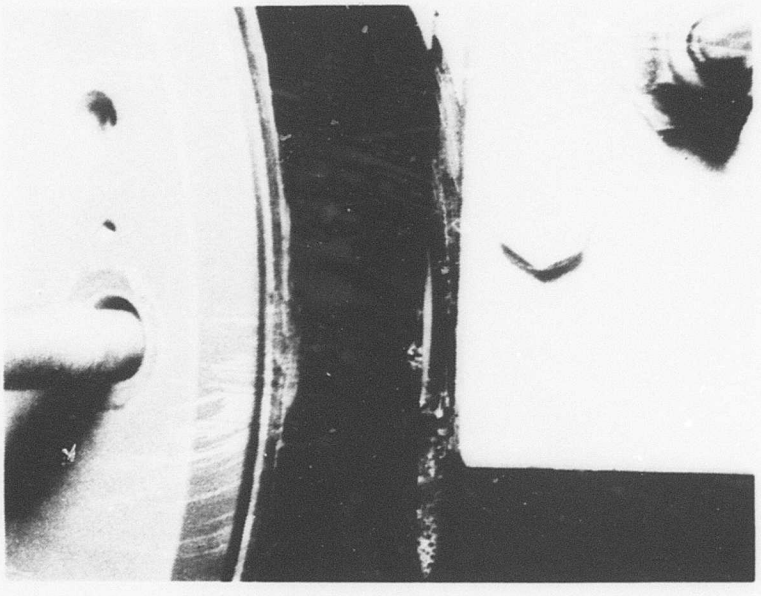

Figure 27. Leak Adjacent to Oil Manifold Pad After Sealing With Fluorinated Silicone.

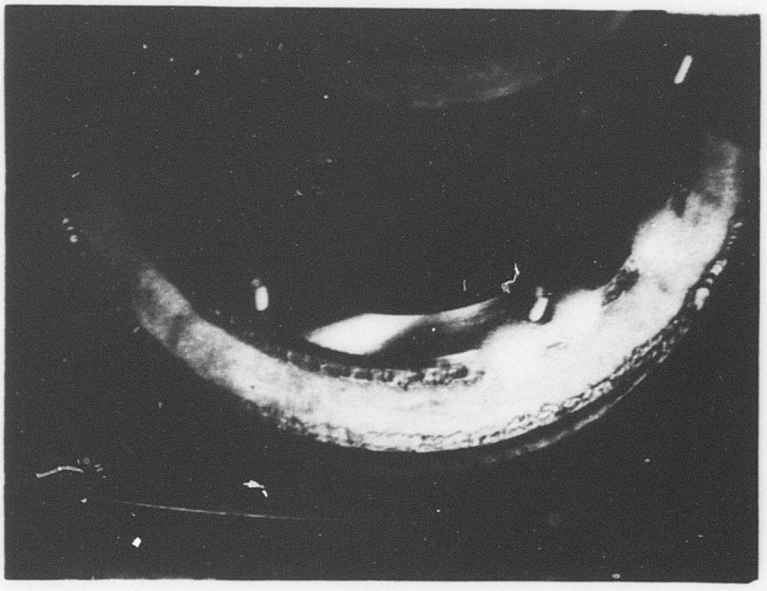

Figure 28. Leaks From Main Bearing Ring Near Top of Housing After Sealing With Fluorinated Silicone.

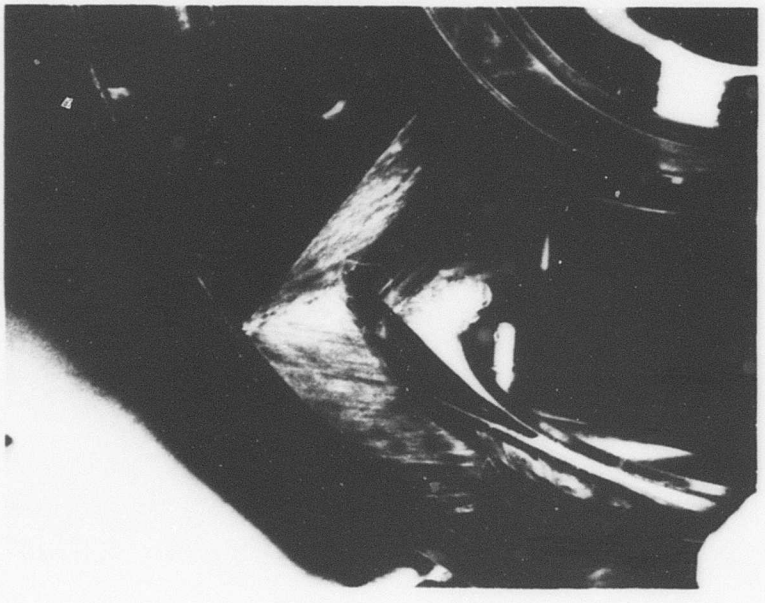

Figure 29. Leak From Main Bearing Ring Near Bottom of Housing After Sealing With Fluorinated Silicone.

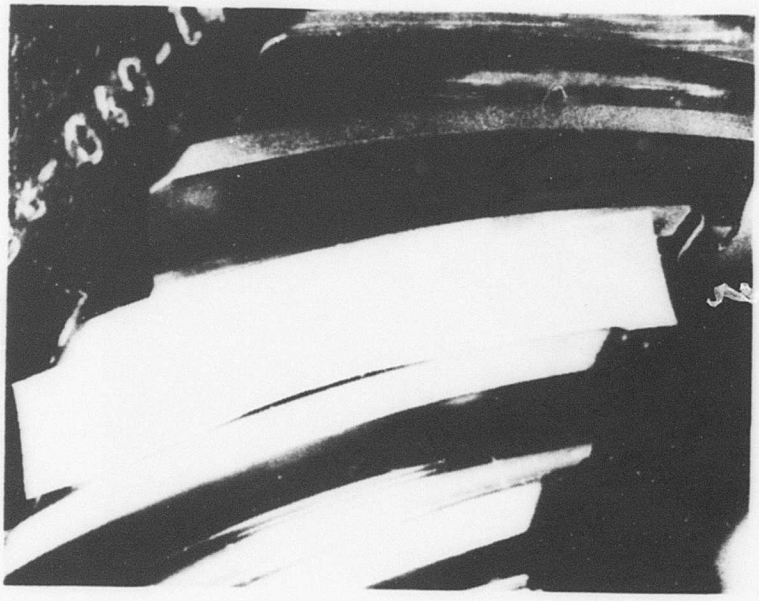

Figure 30. Pinion Drive Side Wear Pattern After 25 Percent (275 HP) Load Step.

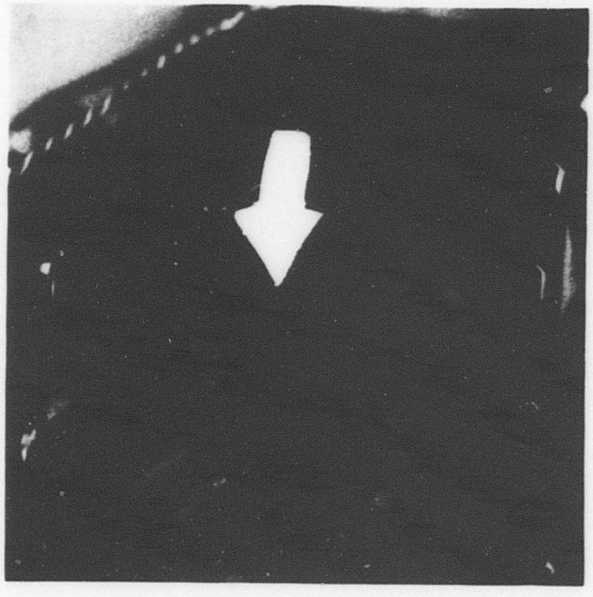

Figure 31. Pinion Drive Side Wear Pattern After 50 Percent (550 HP) Load Step.

Figure 32. Pinion Drive Side Wear Pattern After 75 Percent (825 HP) Load Step.

Figure 33. Pinion Drive Side Wear Pattern After 100 Percent (1100 HP) Load Step.

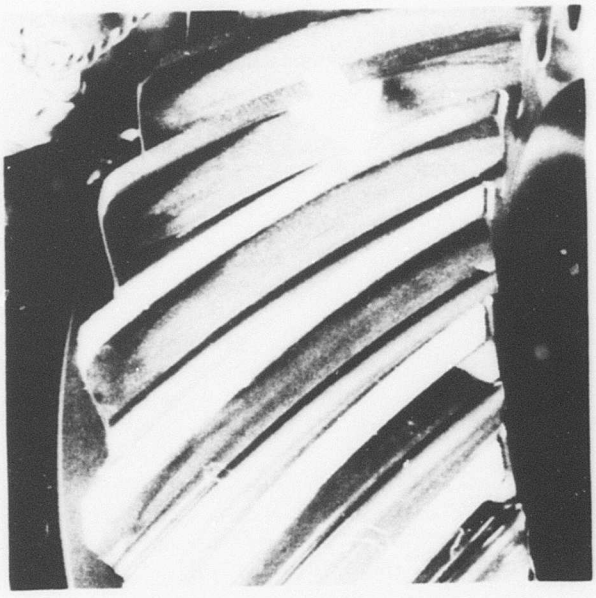

Figure 34. Pinion Drive Side Wear Pattern After 125 Percent (1375 HP) Load Step.

Figure 35. Acceptance Test Wear Pattern for Drive Side of Pinion (1144 Input HP).

stiffer than the magnesium housing since the pattern did not move as close to the heel as usual. The pattern's being slightly low on the tooth could be corrected by changing shim thickness. Since the composite housing was shown to be only slightly stiffer than the magnesium housing, redevelopment of the input spiral bevel pinion and gear was not necessary.

The oil leaks around the input quill increased to a maximum of approximately one quart per hour during the test. Two additional deficiencies were also noted during the test.

The removal and installation of the input quill after each step resulted in the filament-wound carbon-epoxy liner in the input bore splintering as shown in Figure 36. The damaged liner was repaired with Ren Plastic, Inc. RP-1220 epoxy.

As shown in Figure 37, the BMC bearing ring for the forward accessory bore pulled out of the housing approximately .05 inch. The ring-to-housing bond apparently failed. It is not known whether the installation of the offset generator quill during assembly or the vibration during the test caused the failure. The BMC ring around the quill was not carrying any load during the test since the gear was removed from the quill. No repairs were attempted since the failure did not prevent further use of the housing.

THERMAL MAP

The thermal mapping of a transmission using the composite housing was to be performed in two phases. The first phase objectives were to determine the heat rejection rate of the transmission, the weighted sound pressure level of the transmission, and the temperatures of the transmission externally and of the composite housing internally. The second phase objective was to perform a thermal map of the transmission that would have been directly comparable to the thermal map performed under USAAMRDL Contract DAAJ02-72-C-0081.

A test transmission was assembled using the components from S/N A12-52 GFE transmission, the composite housing, an offset generator quill without gear in the forward accessory bore, and a side-mounted generator quill without gear in the right accessory bore. The S/N A12-52 transmission had been used to perform the previous thermal map. The transmission was lubricated with MIL-L-7808. The instrumentation was the same as noted in Reference 1, except for three additional thermocouples bonded to the inside wall of the composite housing opposite thermocouples 1K3, 3K3, and 7K3.

Since the components of S/N A12-52 transmission could possibly have been damaged by the high temperatures experienced

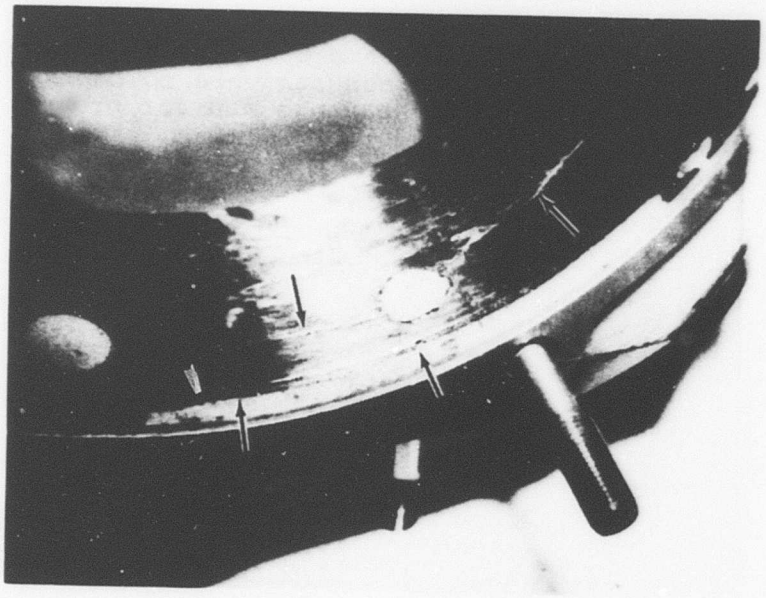

Figure 36. Splintering of Filament-Wound Carbon-Epoxy Liner in Input Quill Bore.

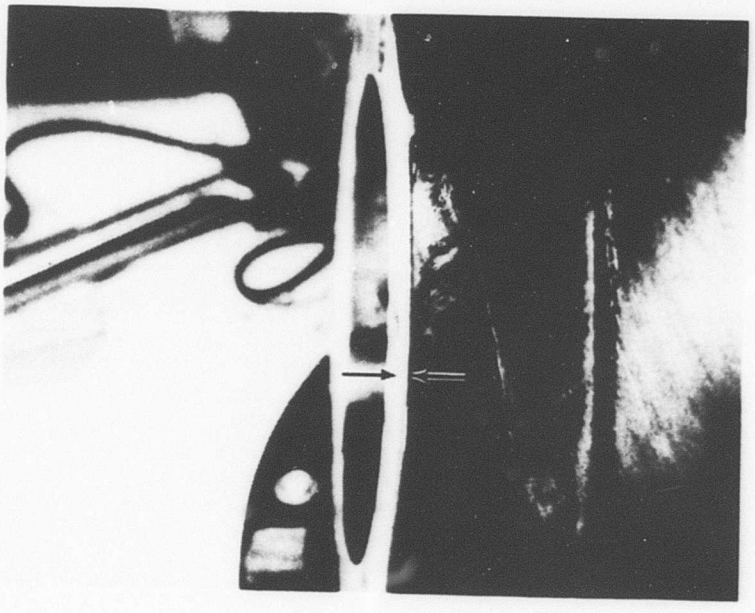

Figure 37. Pullout of Forward Accessory Bore BMC Bearing Ring.

in the previous thermal map, a green run and inspection similar to those outlined in Reference 5 were to be performed. Additional functions of the green run were to check for proper lube system distribution and scavenge and for proper operation of all instrumentation.

The green run schedule shown in Table 5 was successfully completed through Step 13 before stopping for the day.

TABLE 5. GREEN RUN SCHEDULE PRIOR TO THERMAL MAP

STEP	STEP TIME (Hr)	ACCM TIME (Hr)	INPUT RPM	MAST OUTPUT TORQUE (In.-Lb)	MAST OUTPUT HP	T/R DRIVE TORQUE (In.-Lb)	T/R DRIVE HP
1	.1	.1	0-4000	None	None	None	None
2	.1	.2	4400	25,534	87	600	27.6
3	.1	.3	4800	25,534	95	600	30.4
4	.1	.4	5200	25,534	103	600	33.2
5	.1	.5	5800	25,534	116	600	36.0
6	.1	.6	6400	75,000	372	600	39.7
7	.1	.7	7040	135,180	740	600	43.7
8	.1	.8	6600	135,180	693	725	49.0
9	.1	.9	6400	150,000	745	900	59.5
10	.1	1.0	6400	175,000	870	1200	79.4
11	.1	1.1	6400	202,770	1010	450	29.8
12	.2	1.3	6600	195,514	1002	1466	100
13	.1	1.4	6600	207,806	1065	733	50
14	.2	1.6	6600	195,514	1002	1466	100
15	.1	1.7	6600	207,806	1065	733	50
16	.2	1.9	6600	195,514	1002	1466	100
17	.1	2.0	6600	207,806	1065	733	50

After completion of a 10-minute warm-up the following morning, the load was gradually being increased to the torque specified for Step 14. At a load of approximately 1002 mast horsepower and 75 tail rotor horsepower, the input quill area of the composite housing structurally failed. The axial load acting on the input quill at failure was approximately 3600 pounds. As shown in Figures 38 through 41, the input quill was pushed approximately .8 inch out of the housing, allowing the input pinion and gear teeth to disengage. As shown in Figures 42 through 49, the composite housing was damaged beyond repair. Figures 42 and 43 provide orientation for Figures 44 through 49.

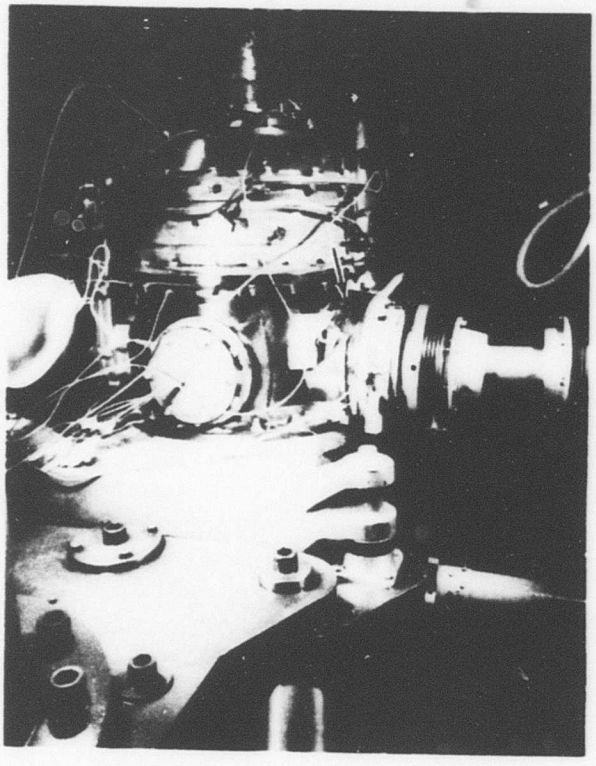

Figure 38. Left-Side View of Transmission After Failure of Composite Housing.

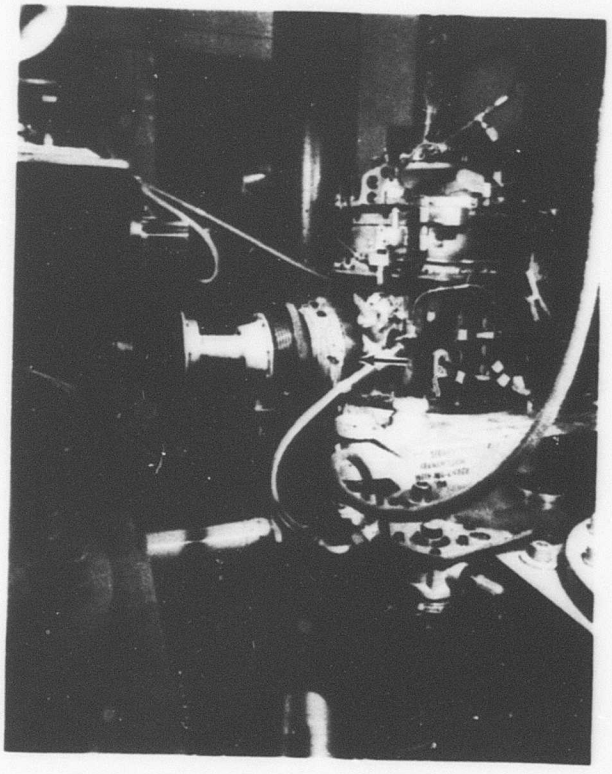

Figure 39. Right-Side View of Transmission After Failure of Composite Housing.

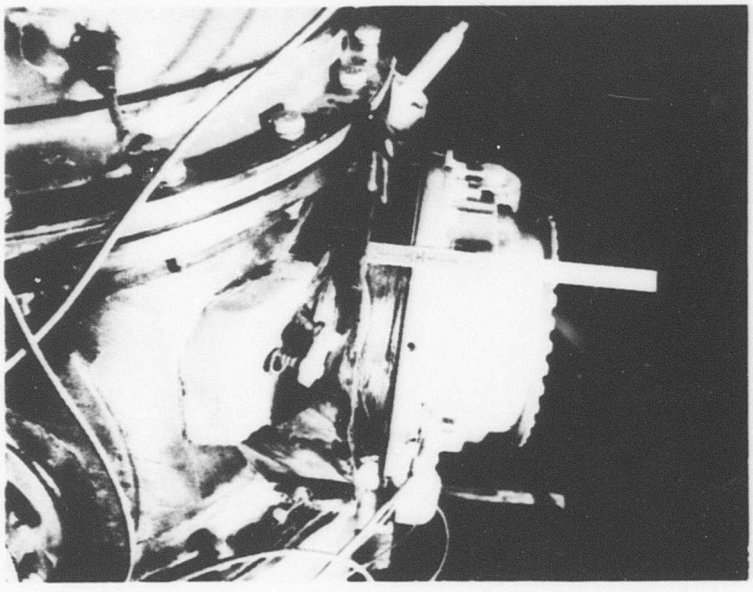

Figure 40. Left-Side View of Composite Housing After Failure.

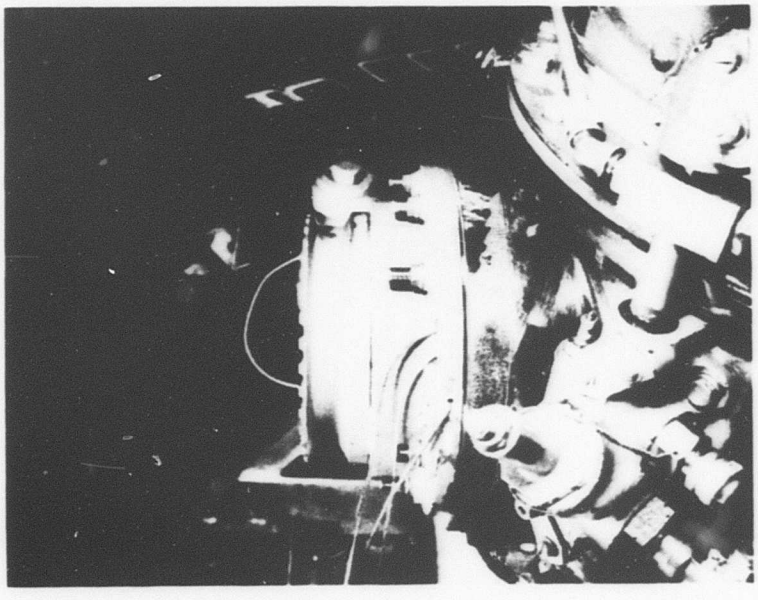

Figure 41. Right-Side View of Composite Housing After Failure.

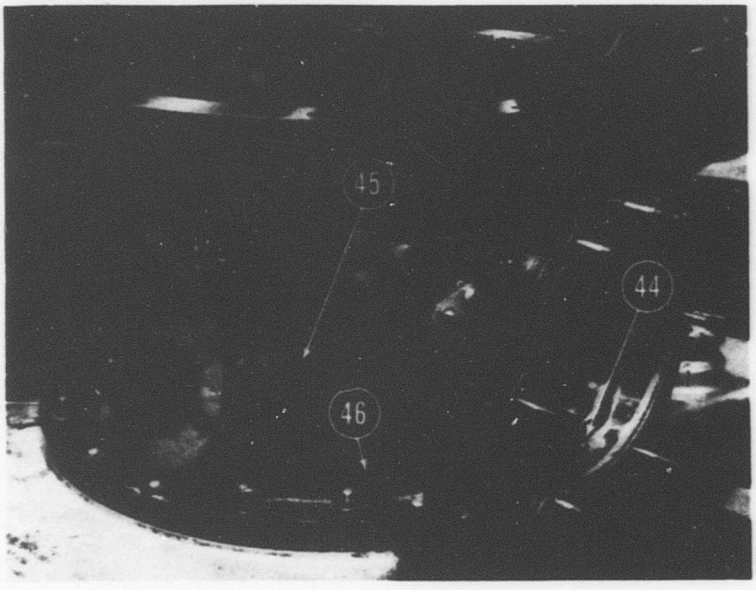

Figure 42. Exterior of Composite Housing After Failure.

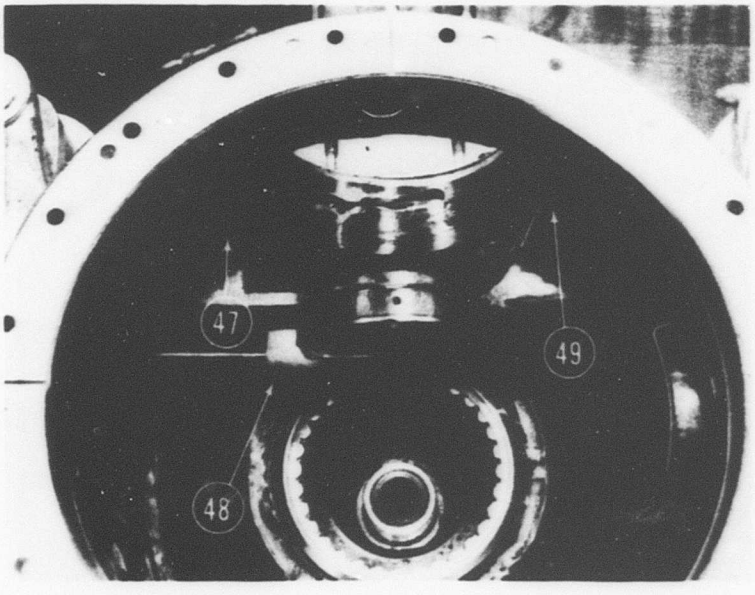

Figure 43. Interior of Composite Housing After Failure.

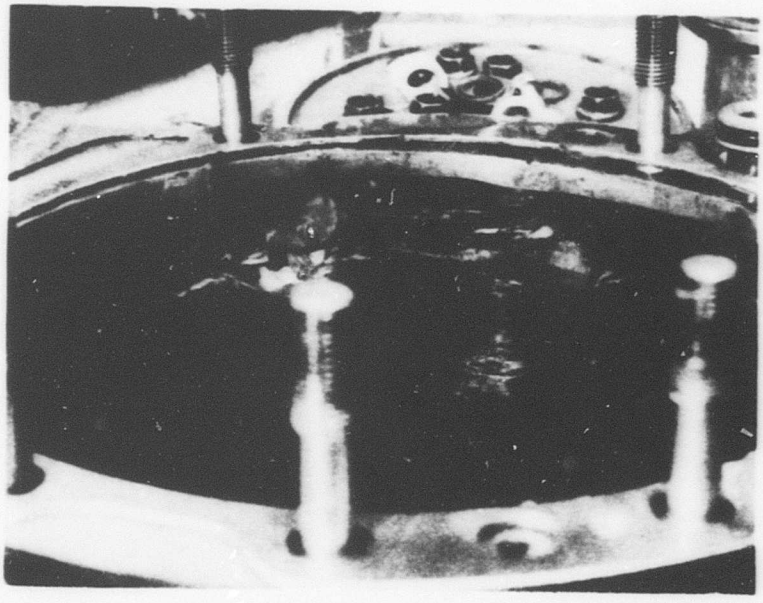

Figure 44. Input Bore of Composite Housing After Failure.

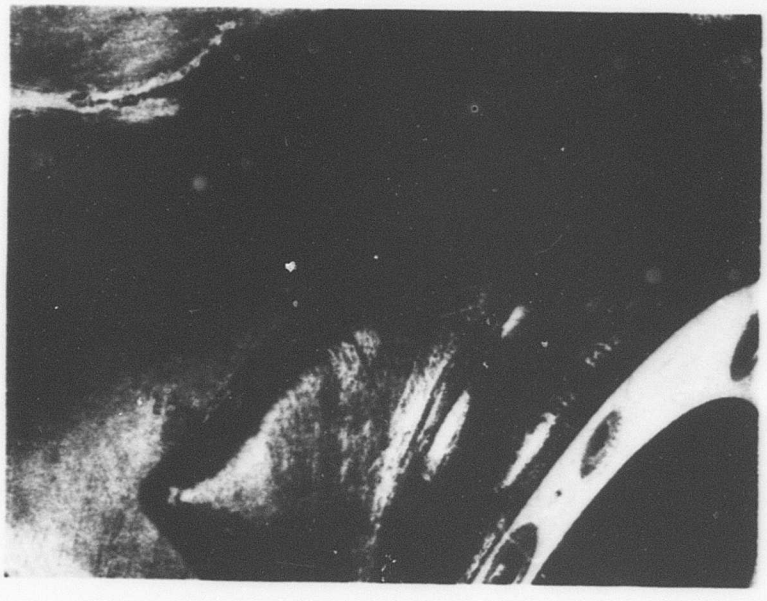

Figure 45. Tear Located on Left Side of Input Bore of Composite Housing After Failure.

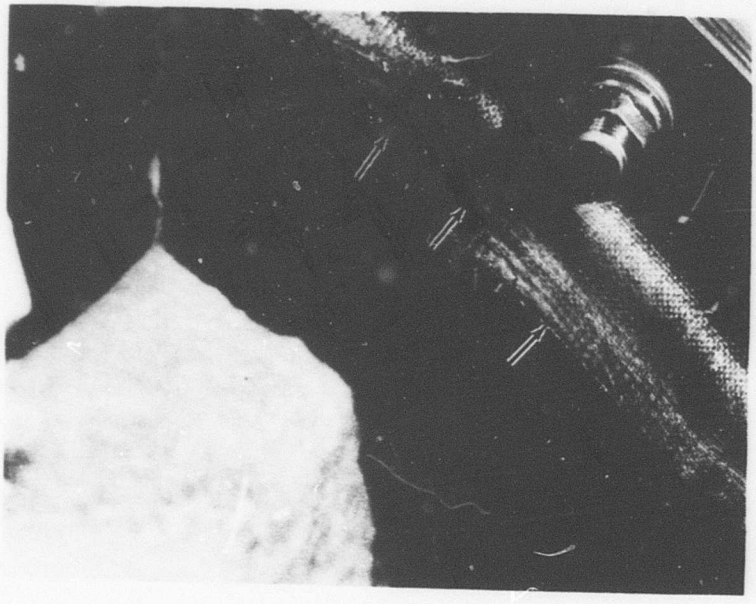

Figure 46. Crack Near Bottom Flange of Composite Housing After Failure.

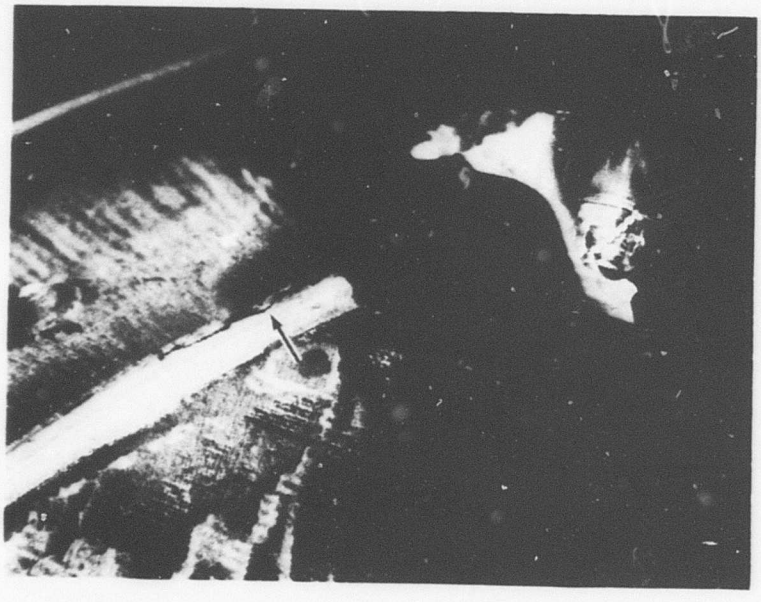

Figure 47. Crack in the Input Pinion Roller Bearing Web-Housing Bond After Failure, Right Side.

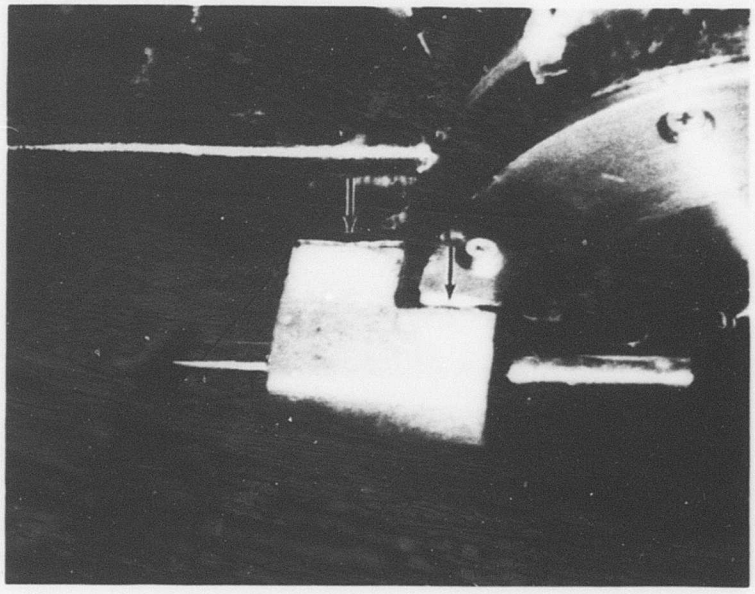

Figure 48. Interior Boss That Houses Oil Jet for Input Pinion Roller Bearing After Failure.

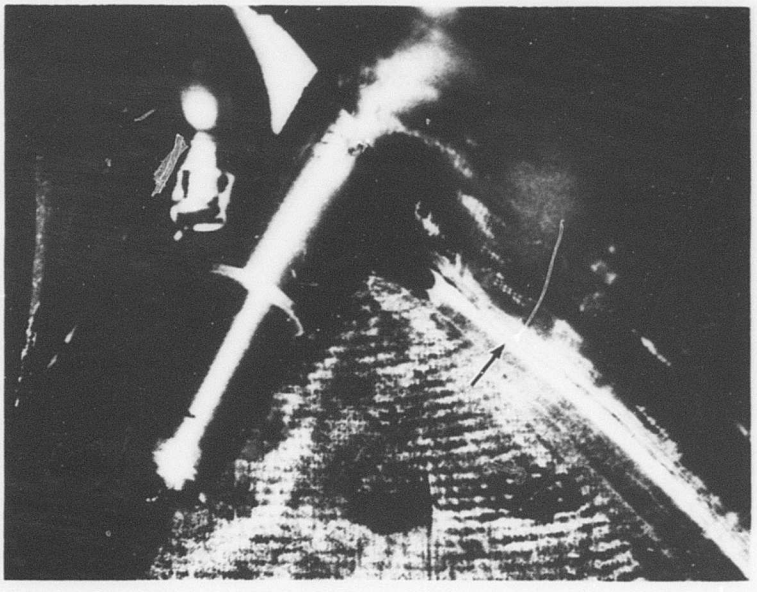

Figure 49. Crack in the Input Pinion Roller Bearing Web-Housing Bond After Failure, Left Side.

FAILURE ANALYSIS

Visual inspection of the failed housing suggested that the failure was probably caused by a faulty bond between the body of the housing and the main bearing ring. Figure 50 shows that the bearing ring pulled out from the housing, the bond material adhered to the bearing ring, and the top of the ring pulled away more than the bottom. The amount of separation varies almost linearly from top to bottom, implying that the origin of failure was at the top. If the applied thrust load had been distributed uniformly around the face of the bearing ring (approximately equal tensile load on each of the 7 mounting studs) at first, then as the top pulled away the lower studs would have become more heavily loaded and the ring would have been loaded in bending perpendicular to its plane. Eventually, this would have caused a failure in combined bending and tension near the bottom of the bearing ring. This failure did in fact occur and is visible in Figures 51 and 52.

An examination of the outer surface of the bearing ring revealed two facts:

1. The adhesive was gold in color rather than the gray characteristic of Hysol Dexter's EA-934.

2. A brown film of material was distributed over approximately 15 percent of the bond material. This substance could be removed from the bond material by hand.

These two phenomena suggested that a large number of voids were probably present at the faying surface between the housing and ring, and these permitted contaminants to contact the EA-934.

Another fact of importance is that the maximum thrust load to which the bearing ring was subjected during any test was 4556 pounds. This compares with the design ultimate thrust load of 8003 pounds per Reference 2.

A test program was performed to either confirm or deny the preliminary assumptions as to the cause of failure. It consisted of the following:

1. The housing was cut in four places along the periphery of the ring, and measurements were made to determine whether the manufactured dimensions were in accordance with those specified on the drawings. The locations at which the housing was cut are shown in Figures 51 and 53, and are marked A-A through D-D.

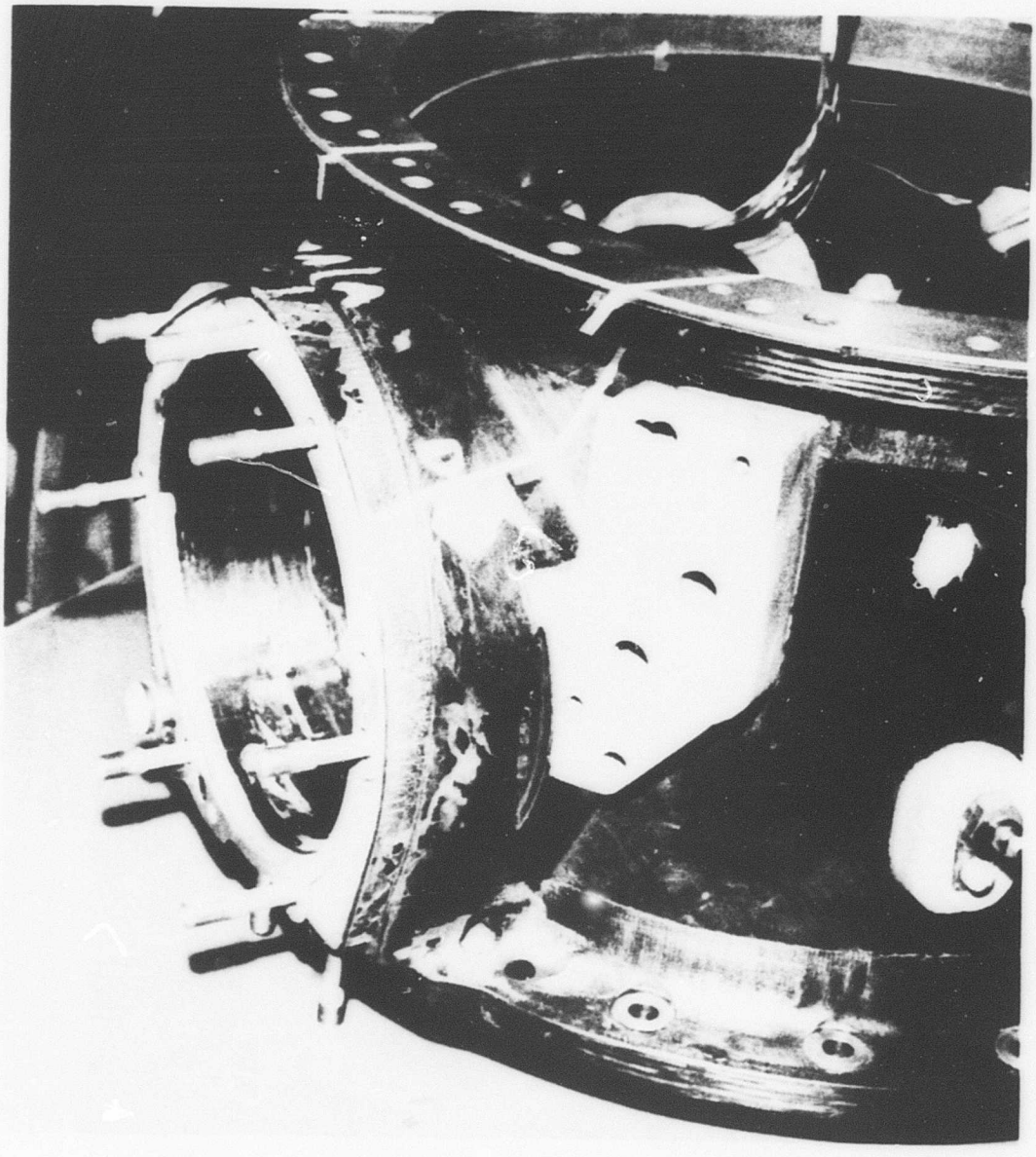

Figure 50. Side View of Failure Showing Bearing Ring Pulled Away From Body of Housing.

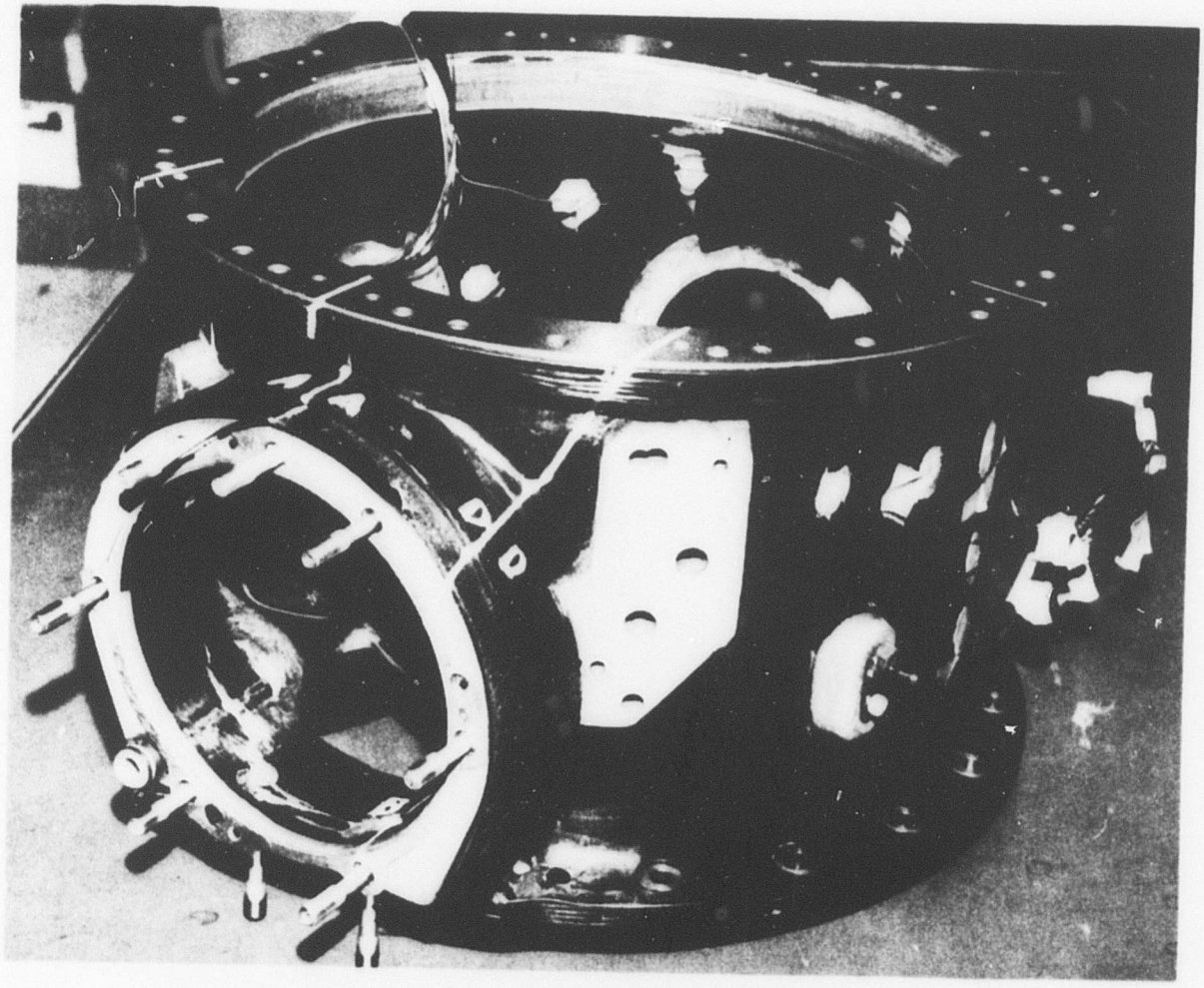

Figure 51. Forward View of Failed Housing Showing Locations at Which Sections Were Cut.

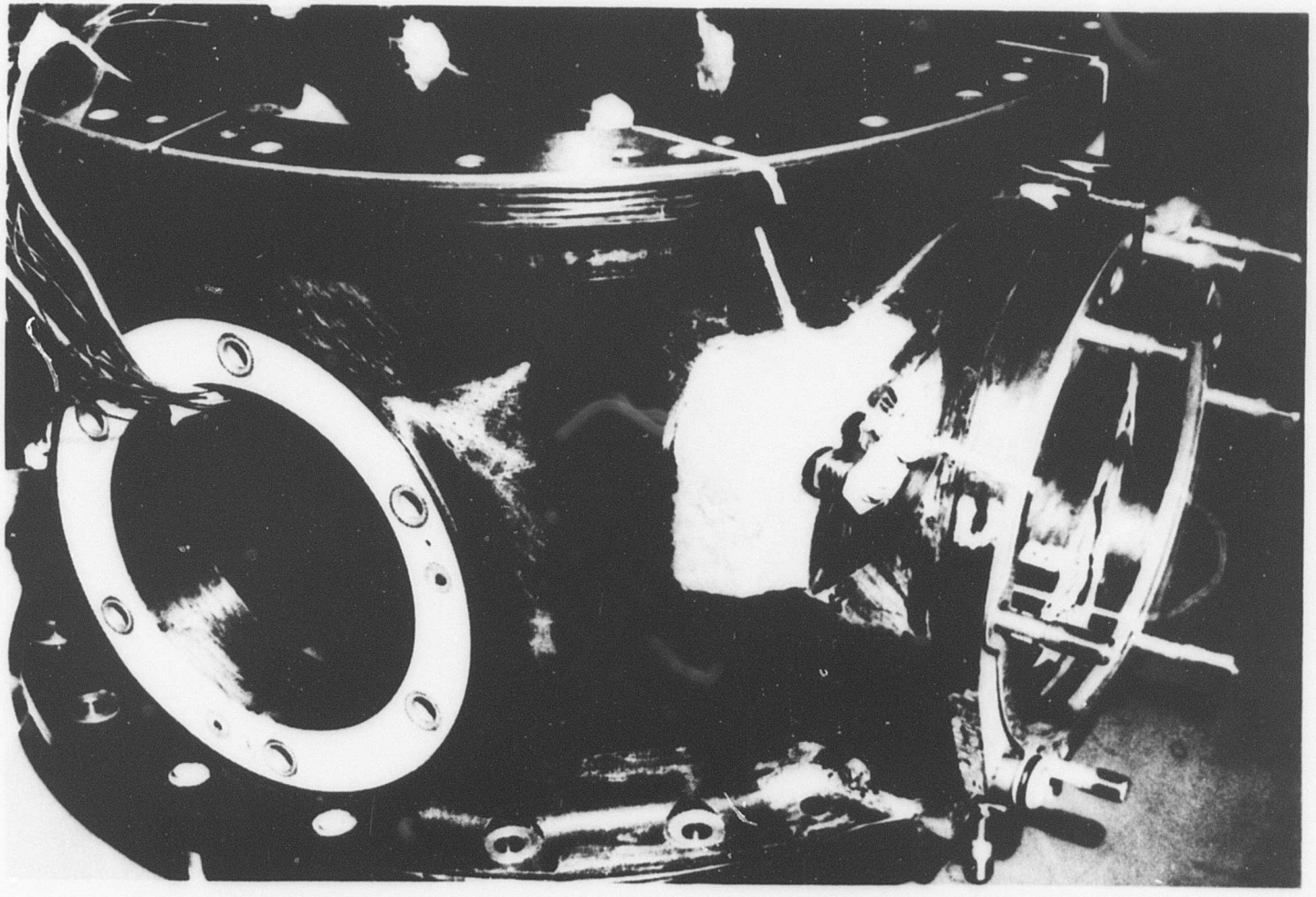

Figure 52. Side View of Failure Showing Locations of Sections A-A, B-B, and C-C.

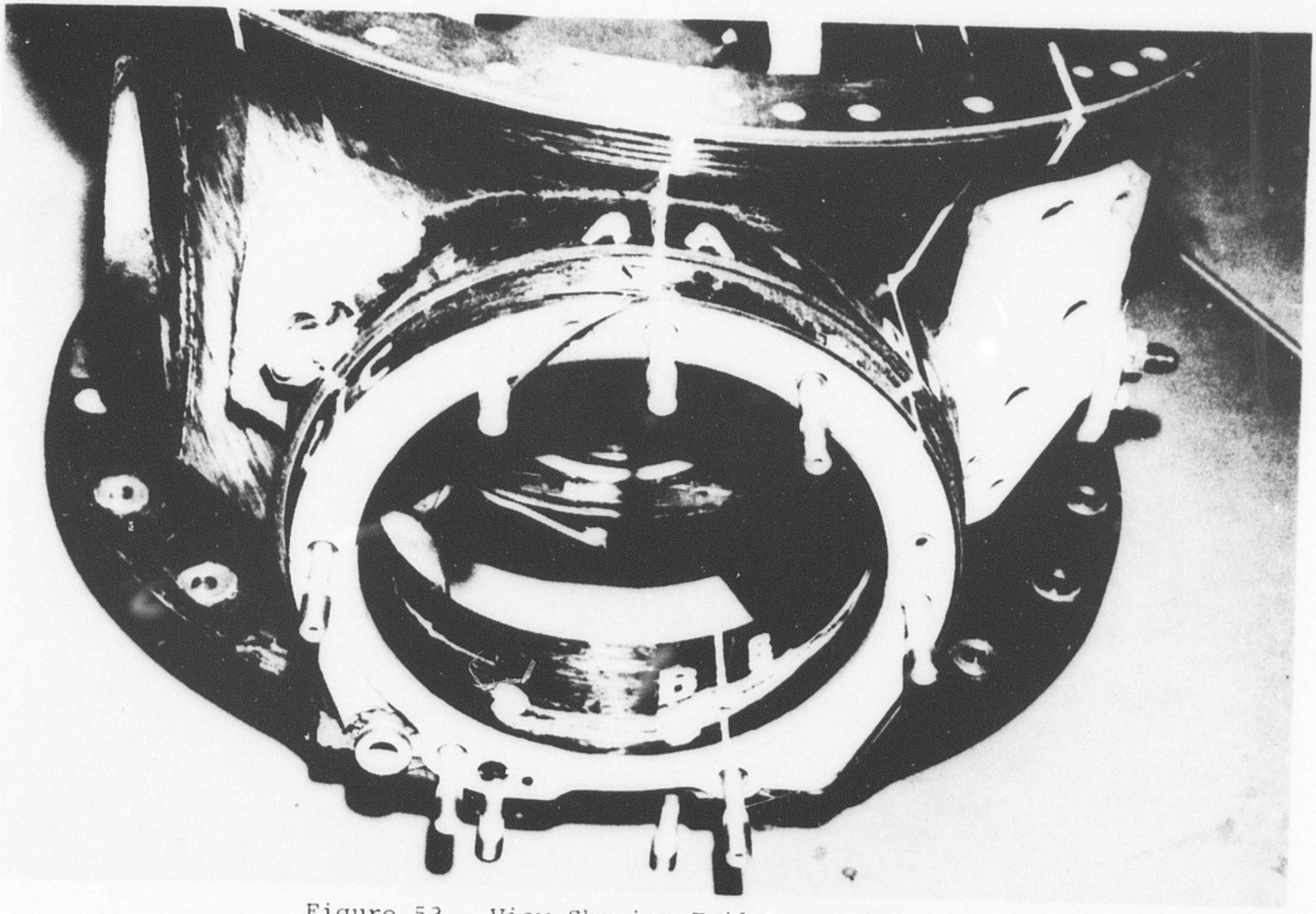

Figure 53. View Showing Failure at Lower Portion of Main Bearing Ring.

2. Five specimens of EA-934 adhesive were bonded to a surface of aluminum alloy and heated to five different temperatures from 150°F to 350°F. Each specimen was maintained at these temperatures for 2 hours. The purpose of this test was to determine if heat would turn the color of the adhesive from gray to gold.

3. Samples of the bond material were removed from the failed section of the case and analyzed by the electron beam microscope and the infrared (IR) spectral photometer. The analysis was compared with a similar analysis made on the basic EA-934 to determine if contaminates were present.

4. Samples of the brown film were removed from the bond and compared with several known materials by means of the IR spectral photometer in order to identify the film.

5. One of the specimens that had been heated to 350°F for 2 hours was placed in the trichloroethylene of a vapor degreaser tank at 180°F to 195°F for 2 hours to determine if this would have any effect on the bond.

6. Six double shear specimens were made by bonding EA-934 to E-glass cloth, two by each of the following procedures:

   - Bond made with contact pressure in accordance with good bonding practice for EA-934 adhesive.

   - Bond made with little or no contact pressure between the glass and adhesive.

   - Bond made with little or no contact pressure between the glass and adhesive; specimens subjected to the vacuum impregnation cycle.

These specimens were then tested in shear to compare the shear strength of EA-934 bonds made with accepted bonding procedures with those made with poor contact pressure and exposed to the vacuum impregnation cycle.

It was virtually impossible to obtain a full set of accurate dimensions on the main bearing ring because the failure had weakened it and the inner ring fell apart when the sections were cut. However, some measurements were made between Sections A-A and D-D as shown in Figure 53. The fore and aft dimensions in line with the thrust load varied from 1.88 to 2.11 inches, as compared with a specified dimension of 2.12.

No tolerances are shown on the drawings of Reference 2. This slight departure from specification was not considered to be significant. The thickness of the filament-wound graphite-epoxy liner in the input quill bore varied from 0.046 to 0.060 inch, as compared with a drawing thickness of 0.12. The size difference was a result of the Modmor I liner being machined to the 204-040-353-23 blueprint dimension. Modmor I is a brittle, notch-sensitive material whose strength could be impaired by machining. The reduced thickness and machining undoubtedly had some weakening effect on the structure, but this probably had little effect on the premature failure. Instead, it may be considered as a minor contributory factor.

The test in which several specimens of EA-934 were heated to several temperatures up to 350°F showed essentially nothing. The specimen exposed to 350°F showed a small discoloration tending toward a green-gold color. To see if the change was cumulative with time, this specimen was reheated and the temperature maintained for 3 more hours. No further discoloration resulted. The color was far from the gold color seen in the failed adhesive. It was concluded, therefore, that something other than heat caused the adhesive's discoloration.

The analysis of the bond surface by the electron beam microscope showed traces of silicon, chlorine, and magnesium in addition to the materials contained in uncontaminated EA-934. The presence of these materials can be explained in that silicon is one of the materials used in the impregnation process, chlorine is one of the elements of the trichloroethylene degreaser, and the upper case is made from magnesium. Therefore, traces of magnesium could go into the solution in the transmission oil and flow into the bond. The probability of these materials' appearing on the bond surface is increased if the bond is not sealed at the edges--characteristic of a bond with a large number of voids.

Although it was suspected that transmission oil permeated the bond surface, its presence could not be detected because the degreaser removed all traces of oil. The presence of magnesium, however, does lend strong support to the theory that there was oil at the faying surface between the case and the bearing ring.

The IR spectral photometer verified the results obtained with the electron beam microscope, and added one important piece of information: the brown film found on approximately 15 percent of the adhesive surface was a polyester material. Figure 54 shows the traces of the comparison of the brown film with a known polyester. The two materials follow each other closely throughout the range of wavelengths tested. Since a polyester material was used to impregnate the housing at 85 to 100 psi

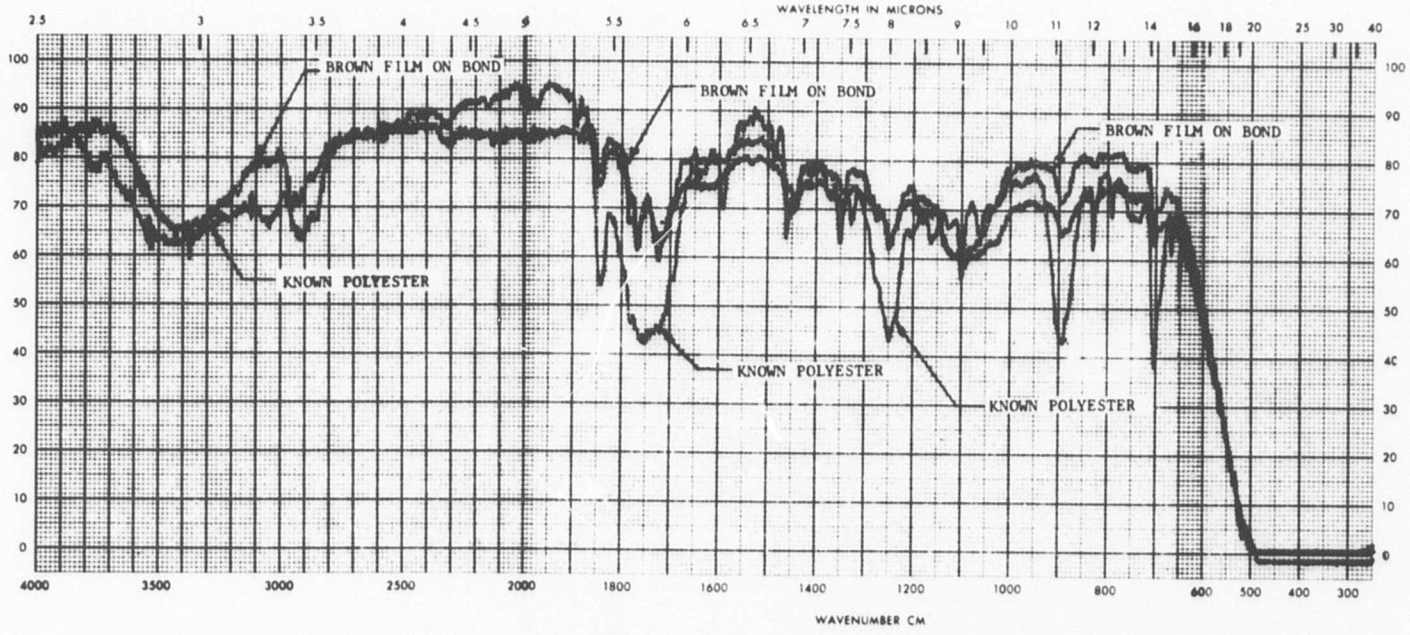

Figure 54. Infrared Spectral Photometer Traces Showing Comparison of Brown Film Found on Bond Surface With Known Polyester Material.

pressure, this must have been deposited during the impregnation cycle. The polyester would have penetrated such a large area of the adhesive only if there had been large voids in the bond.

The test of the EA-934 specimen, initially heated to 350°F, in the vapor degreaser tank failed to reveal any signs of bond deterioration. The bond surface appeared as smooth as before the test, even under magnification. It is concluded that the trichloroethylene degreaser did not chemically attack the EA-934.

TABLE 6. RESULTS OF DOUBLE SHEAR TESTS OF EA-934 BONDED TO FIBERGLASS CLOTH

Type of Specimen	Failing Shear Stress	Average of 2 Tests	Relative Average Strength
Good bond practice	1475 1755	1615	1.0
Minimal contact pressure	1619 992	1305	.81
Minimal contact pressure plus impregnation	1294 1485	1390	.86

Although the test results show a relatively large scatter, there is a 14 to 19 percent reduction in strength between specimens made with good bonding practice (firm pressure between adherents) and those in which minimal bonding pressure was used. The impregnation process did not have an adverse effect on the bond shear strength. However, the failed specimens did not have any of the brown film that was found on the failed part. It may therefore be reasonably assumed that the test bonds were of better quality than the one made on the transmission case. It is also assumed that, although they had less strength than the good test bond, they were stronger than the one made on the case.

The laboratory tests confirm that the primary failure was in the bond between the main bearing ring and the body of the housing; and the cause of the failure at low load was the poor quality of the bond. The origin of failure was at the upper portion of the ring, with failure progressing from top to bottom. The final failure was one of combined tension and out-of-plane bending of the bearing ring. Although a poor quality bond was the cause of premature failure, one cannot say with certainty that it would have survived if the bond had been

perfect. It has never been proven that with a perfect bond the structure would be adequate for the design ultimate load of 8003 pounds.

CONCLUSIONS

The testing of the composite material helicopter transmission housing led to the following conclusions:

1. This particular composite material transmission housing design does not have the structural integrity to be used in a helicopter transmission. The design has many shortcomings, the most serious being the structural failure of the input quill area of the housing due primarily to a defective main bearing ring-to-housing bond. The defective bond was evidenced by oil leaking through the bond prior to the spiral bevel gear development test; the presence of silicon, chlorine, magnesium, and the resin used in the vacuum impregnation process throughout the bond interface; and the reduced load-carrying capacity of double lap shear specimens bonded together with no pressure.

2. The composite material housing has very poor thermal conductivity properties. The average thermal conductivity of the composite housing was .52 BTU/hr-ft-^{0}F for 141^{0}F to 203^{0}F. For comparison, the thermal conductivity of magnesium and asbestos is 92 BTU/hr-ft-^{0}F and .087 to .375 BTU/hr-ft-^{0}F, respectively. The composite housing would conduct .6 percent as much heat as the magnesium housing. The low thermal conductivity of the composite housing would result in increasing the lube system capacity with an accompanying increase in weight to maintain the transmission oil temperature in the 200^{0}F - 230^{0}F temperature range. Unless a transmission is developed with components capable of operating at a higher temperature, possibly in the 400^{0}F temperature range, an increase in lube system capacity would be required. quired.

3. The composite housing, especially the carbon-epoxy material, is more difficult to machine than conventional magnesium or aluminum housings. Grinding had to be used almost entirely to machine the carbon-epoxy material.

4. The average coefficient of linear thermal expansion of the filament-wound carbon-epoxy liners in the housing bores in the circumferential direction was 2.0 x 10^{-6} in./in.-^{0}F for 123^{0}F to 350^{0}F. For comparison, the coefficient of linear thermal expansion of steel and magnesium is 6.3 x 10^{-6} in./in.^{0}F and 14.0 x 10^{-6}, respectively. The coefficient of linear thermal

expansion of the liners in the axial direction varied from 8.2×10^{-6} in./in.-^{0}F at 130^{0}F to 16.9 in./in.-^{0}F at 250^{0}F.

5. The spiral bevel gear development test showed that the S/N 2 composite housing was slightly stiffer than the magnesium housing since the wear pattern on the input spiral bevel pinion teeth did not move as close to the heel as usual. However, the S/N 2 composite housing is approximately two pounds heavier than a magnesium housing.

6. The choice of materials for the housing has to be questioned. Modmor I, as is characteristic of HM graphite, is brittle, has low fracture toughness, and has little structural forgiveness. Although Modmor I has high stiffness, it is not recommended for use where vibration, frequent heat cycling, and high cyclic loadings are design considerations. The bulk molding compound (BMC) was selected for its machinability properties. However, it cannot be substituted equally for cast magnesium or aluminum due to its inferior strength. The filament-wound carbon-epoxy liners have very poor axial strength, as exhibited by circumferential cracks in the liners and splintering of the fibers during assembly and removal of the gear quills. Additionally, the difference between the coefficients of thermal expansion of carbon-epoxy and BMC could possibly have contributed to the failure of the ring-to-housing bonds.

RECOMMENDATIONS

The following recommendations are made for future applications of composite materials to transmission housings:

1. Composite materials should be investigated further for less complex applications such as airframe attachment housings and transmission oil sumps. The airframe attachment housings have less demanding machining requirements, less complex loading, fewer oil passages, and less effect on heat transfer, since in many applications they do not closely surround gears. Oil sumps made of composite materials are presently being manufactured and developed for helicopter transmissions.

2. Future designs should not contain a joint whose integrity relies on an unpressurized cold bond such as that attaching the bearing ring to the body of the housing. One can never be certain that the two faying surfaces are well matched dimensionally. When one ring is nested into another, there is a tendency for the adhesive to wipe away, to form local high and low spots, and consequently to develop large voids. The joint should at least be the type of structure capable of being expanded by male tooling to assure that the bond is made with uniform pressure and heat. Furthermore, it is recommended that the joint configuration be flanged so that a bond in shear is not solely relied upon to carry the axial gear load.

3. Prior to the fabrication of future composite housings, a test program should be conducted to verify the strength of joints and to insure that all materials have compatible thermal expansion characteristics.

4. Either Type II (HT) or Type A graphite should be considered for future designs. Although high stiffness was a design requirement and the housing would have been heavier if Type II or Type A had been used, the operational environment for a transmission housing is too severe for as brittle a material as Type I (HM) graphite.

REFERENCES

1. Drennan, J. H., and Walker, R. D., TRANSMISSION THERMAL MAPPING (UH-1 MAIN ROTOR TRANSMISSION), USAAMRDL Technical Report 73-90, Eustis Directorate, U. S. Army Air Mobility Research and Dvelopment Laboratory, Fort Eustis, Virginia, December 1973, AD 777803.

2. Chase, V. A., INVESTIGATION OF THE USE OF CARBON COMPOSITE MATERIALS FOR HELICOPTER TRANSMISSION HOUSING APPLICATIONS, USAAMRDL Technical Report 73-7, Eustis Directorate, U. S. Army Air Mobility Research and Development Laboratory, Fort Eustis, Virginia, July 1973, AD 771978.

3. Weber, R. L., White, M. W., and Manning, K. V., COLLEGE PHYSICS, 3rd Edition, New York, McGraw-Hill Book Company, 1959.

4. Kreith, F., PRINCIPLES OF HEAT TRANSFER, 2nd Edition, Scranton, Pennsylvania, International Textbook Company, 1966.

5. Hopfensperger, L. J., SPECIFICATION FOR THE 204-040-009, 204-040-016, AND 205-040-001 TRANSMISSION ASSEMBLIES, BHC Report 204-947-153, Bell Helicopter Company, Fort Worth, Texas, February 1964.

APPENDIX A
CALCULATIONS FOR THERMAL EXPANSION ANALYSIS

AVERAGE COEFFICIENT OF THERMAL EXPANSION IN THE CIRCUMFERENTIAL DIRECTION

$$\bar{\alpha}_H = \frac{1}{n}\sum_{r=1}^{n} \alpha_r = \frac{179.2 \times 10^{-6} \text{ in./in.-}^0\text{F}}{91}$$

$$= 2.0 \times 10^{-6} \text{ in./in.-}^0\text{F}$$

Values of α are from Tables A-1 and A-2.

INTERFERENCE FIT OF BEARING LINERS

Select a line-to-line fit at -40° F.

$$D_{L_{-40}} = D_{L_{70}} \left[1 + \alpha_L \Delta T\right]$$

$$D_{H_{-40}} = D_{H_{70}} \left[1 + \bar{\alpha}_H \Delta T\right]$$

$$D_{H_{-40}} = D_{L_{-40}}$$

$$D_{H_{70}} \left[1 + \bar{\alpha}_H \Delta T\right] = D_{L_{70}} \left[1 + \alpha_L \Delta T\right]$$

$$D_{H_{70}} = \frac{D_{L_{70}} \left[1 + \alpha_L \Delta T\right]}{\left[1 + \bar{\alpha}_H \Delta T\right]}$$

$$= \frac{D_{L_{70}} \left[1 + (6.3 \times 10^{-6} \text{ in./in.-}^0\text{F})(-40^0\text{F} - 70^0\text{F})\right]}{\left[1 + (2.0 \times 10^{-6} \text{ in./in.-}^0\text{F})(-40^0\text{F} - 70^0\text{F})\right]}$$

$$D_{H_{70}} = .999527\ D_{L_{70}}$$

For the input pinion roller bearing liner,

$$D_{H_{70}} = (.999527)(3.7545) = 3.7527$$

$$I = 3.7545 - 3.7527 = .0018 \text{ (use } .0020 \pm .0002)$$

Machine housing bore to 3.7525 ±.0002.

TABLE A-1. COEFFICIENT OF THERMAL EXPANSION, TEST 1

LOCATION	GAGE NO.	DIRECTION	COEFFICIENT OF EXPANSION AT SEVEN DIFFERENT TEMPERATURES - (In./In.-°F) x 10^6						
			123°F	150°F	200°F	250°F	300°F	325°F	350°F
Forward Accessory Bore	3	Cir	2.1	2.0	2.0	1.8	1.5	1.3	1.1
	4	Cir	2.7	2.8	2.7	2.5	2.1	1.9	1.7
	5	Axial	8.7	9.5	---------- off scale ----------				
Left Accessory Bore	6	Axial	9.8		---------- off scale ----------				
	7	Cir	2.3	2.3	2.2	2.1	1.8	1.7	1.6
Input Pinion Roller Bearing Bore	9	Cir	3.6	3.9	3.5	3.8	4.2	4.3	4.4
	10	Cir	---------- Gage Failure ----------						
	11	Axial	9.0	9.9	---------- off scale ----------				
Input Quill Bore	12	Axial	9.6	10.5	---------- off scale ----------				
	13	Cir	1.7	1.6	1.5	1.4	1.3	1.3	1.4
	14	Cir	1.7	1.6	1.6	1.4	1.1	1.1	1.1
Input Gear Roller Bearing Bore	15	Cir	1.8	1.7	1.4	1.2	1.1	1.2	1.1

TABLE A-2. COEFFICIENT OF THERMAL EXPANSION, TEST 2

LOCATION	GAGE NO.	DIRECTION	COEFFICIENT OF EXPANSION AT SIX DIFFERENT TEMPERATURES (In./In.-°F) x 10^6					
			130°F	150°F	200°F	250°F	300°F	350°F
Forward Accessory Bore	3	Cir	1.6	2.5	2.0	1.9	1.6	1.2
	5	Axial	8.2	9.2	10.8	-------Off Scale-------		
Left Accessory Bore	6	Axial	10.0	10.7	----------Off Scale----------			
	7	Cir	2.3	2.5	2.3	2.2	2.0	1.7
	8	Cir	2.3	2.4	2.1	2.0	1.8	1.6
Input Pinion Roller Bearing Bore	9	Cir	3.3	2.2	2.1	3.0	4.0	4.8
	10	Cir	----------Gage Failure----------					
	11	Axial	9.1	9.6	11.5	15.9	--Off Scale---	
Input Quill Bore	12	Axial	9.4	10.0	11.7	16.9	--Off Scale---	
	13	Cir	1.7	1.7	1.6	1.6	1.5	1.5
	14	Cir	1.5	1.5	1.5	1.3	0.8	0.6
Input Gear Roller Bearing Bore	15	Cir	1.6	1.4	1.4	1.2	1.0	1.2

For the input gear roller bearing liner,

$D_{H_{70}}$ = .999527 (6.7130) = 6.7098

I = 6.7130 - 6.7098 = .0032 (use .0035 ±.0003)

Machine housing bore to 6.7095 ±.0003.

APPENDIX B
CALIBRATION DATA FOR THERMAL CONDUCTIVITY ANALYSIS

The temperature-sensitive strain gages were located as shown in Figure 19. Nine gages (two each at four separate locations, and an ambient)were used. Locating the gages in pairs directly opposite each other and using a matching network, the oscillograph deflection represented the temperature differences across the wall. The objective of the calibration procedure was to determine the slope of the linear curve defining the variation of the temperature difference versus oscillograph deflection.

Calibration was performed by replacing one gage of each pair with a 49.8-ohm resistor which represented a constant 73°F reference temperature. The instrumented housing was then placed in the oven, and the oscillograph deflection of the remaining gage was determined at four different temperatures. The resulting data is shown in Table B-1.

TABLE B-1. CALIBRATION DATA FOR THERMAL CONDUCTIVITY ANALYSIS

TEMP - T (°F)	OSCILLOGRAPH DEFLECTION - Δ(IN.)			
	Gages 1 and 2	Gages 3 and 4	Gages 5 and 6	Gages 7 and 8
73	0.00	0.00	0.00	0.00
118	3.67	3.89	3.75	3.60
128	4.37	4.62	4.42	4.30
141	5.13	5.54	5.28	5.10
148	5.63	6.08	5.75	5.60

By using these data points and Bell Helicopter's computer program nesd10 for curve fitting by the least-squares method, the best-fitting linear curve and corresponding equations were determined for the four pairs of strain gages. The four equations are:

$T = 71.9 + 13.2\Delta$ For gages 1 and 2

$T = 72.2 + 12.3\Delta$ For gages 3 and 4

$T = 72.0 + 12.9\Delta$ For gages 5 and 6

$T = 72.1 + 13.3\Delta$ For gages 7 and 8

The slope of each curve was then determined by differentiating the corresponding equation by $d\Delta/dt$.

$d\Delta/dt = 13.2$	For gages 1 and 2
$d\Delta/dt = 12.3$	For gages 3 and 4
$d\Delta/dt = 12.9$	For gages 5 and 6
$d\Delta/dt = 13.3$	For gages 7 and 8

Removing the 49.8-ohm resistor and reconnecting the second gage readied the setup for the thermal conductivity test. The temperature difference across each wall thickness was determined by multiplying the amount of oscillograph deflection by the slope. Calculations for the thermal conductivity analysis are shown in Appendix C.

APPENDIX C
CALCULATIONS FOR THERMAL CONDUCTIVITY ANALYSIS

TEMPERATURE DIFFERENCE ACROSS WALL

$$\Delta T = (d\Delta/dt)(\Delta)$$

The $d\Delta/dt$ values are from Appendix B and the Δ values are from Table C-1. Subscripts denote the temperature at which the test was conducted.

For gages 1 and 2 on port accessory bore asbestos:

$$\Delta T_{203} = (13.2^{0}F/in.)(1.26\ in.) = 16.6^{0}F$$

$$\Delta T_{193} = (13.2^{0}F/in.)(1.30\ in.) = 17.2^{0}F$$

$$\Delta T_{141} = (13.2^{0}F/in.)(.63\ in.) = 8.3^{0}F$$

For gages 3 and 4 on housing wall:

$$\Delta T_{203} = (12.3^{0}F/in.)(.34\ in.) = 4.2^{0}F$$

$$\Delta T_{193} = (12.3^{0}F/in.)(.32\ in.) = 3.9^{0}F$$

$$\Delta T_{141} = (12.3^{0}F/in.)(.21\ in.) = 2.6^{0}F$$

For gages 5 and 6 on housing wall:

$$\Delta T_{203} = (12.9^{0}F/in.)(.24\ in.) = 3.1^{0}F$$

$$\Delta T_{193} = (12.9^{0}F/in.)(.20\ in.) = 2.6^{0}F$$

$$\Delta T_{141} = (12.9^{0}F/in.)(.05\ in.) = .6^{0}F$$

TABLE C-1. OSCILLOGRAPH DEFLECTIONS REPRESENTING TEMPERATURE DIFFERENCE ACROSS WALL

TEMP - T (^{0}F)	OSCILLOGRAPH DEFLECTION - Δ(IN.)			
	Gages 1 and 2	Gages 3 and 4	Gages 5 and 6	Gages 7 and 8
203	1.26	0.34	0.24	2.16
193	1.30	0.32	0.20	1.94
141	0.63	0.21	0.05	1.16

For gages 7 and 8 on asbestos top cover:

$$\Delta T_{203} = (13.3^{0}F/in.)(2.16\ in.) = 28.7^{0}F$$

$$\Delta T_{193} = (13.3^{0}F/in.)(1.94\ in.) = 25.8^{0}F$$

$$\Delta T_{141} = (13.3^{0}F/in.)(1.16\ in.) = 15.4^{0}F$$

AREA CALCULATIONS

Logarithmic mean area of housing wall:

$$\bar{A}_H = (A_o - A_i)/\ln (A_o/A_i)$$

$$A_o = \pi D_o h = \pi(14.74\ in.)(8.95\ in.) = 414.4\ in.^2$$

$$A_i = \pi D_i h = \pi(14.40\ in.)(8.95\ in.) = 404.9\ in.^2$$

$$\bar{A}_H = (414.4\ in.^2 - 404.9\ in.^2)/\ln (414.4\ in.^2/404.9\ in.^2)$$

$$\bar{A}_H = 409.6\ in.^2$$

Area of top asbestos cover:

$$A_{A_T} = \pi(D_T/2)^2 = \pi(13.75\ in./2)^2 = 148.5\ in.^2$$

Area of bottom asbestos cover:

$$A_{A_B} = \pi(D_B/2)^2 = \pi(14.25\ in./2)^2 = 159.5\ in.^2$$

Area of asbestos plug in input bore:

$$A_{A_I} = \pi(D_I/2)^2 = \pi(6.75\ in./2)^2 = 35.8\ in.^2$$

Area of asbestos plugs in forward and port accessory bores:

$$A_{A_F} = A_{A_P} = \pi(D_F/2)^2 = \pi(5.00\ in./2)^2 = 19.6\ in.^2$$

THERMAL CONDUCTIVITY CALCULATIONS

$$Q_T = Q_A + Q_C$$

which expands to

$$Pt = \left[k_A\left(A_{A_T} + A_{A_B}\right)\Delta T_{A_T}/\Delta L_A + K_A\left(A_{A_F} + A_{A_P} + A_{A_I}\right)\right.$$
$$\left.\Delta T_{A_P}/\Delta L_A\right] + \left[k_H\ \bar{A}_H\ \overline{\Delta T}_H/\Delta r_H\right]$$

Solving for k_H,

$$k_H = \left[\Delta r_H/\bar{A}_H\overline{\Delta T}_H\right]\left[Pt - k_A\left(A_{A_T} + A_{A_B}\right)\Delta T_{A_T}/\Delta L_A\right.$$
$$\left. - k_A\left(A_{A_F} + A_{A_P} + A_{A_I}\right)\Delta T_{A_P}/\Delta L_A\right]$$

$$k_H = \left[(.17\text{ in.})(12\text{ in./ft})/(409.6\text{ in.}^2)\ \overline{\Delta T}_C\right]$$
$$\left[(1500\text{ watt})(3.413\text{ BTU/watt-hr})t\right.$$
$$- (.375\text{ BTU/hr-ft-}^0\text{F})(148.5\text{ in.}^2 + 159.5\text{ in.}^2)$$
$$\Delta T_{A_T}/(1\text{ in.})(12\text{ in./ft}) - (.375\text{ BTU/hr-ft-}^0\text{F})$$
$$(19.6\text{ in.}^2 + 19.6\text{ in.}^2 + 35.8\text{ in.}^2)\Delta T_{A_P}/(1\text{ in.})$$
$$\left.(12\text{ in./ft})\right]$$

$$k_H = \left[(.005/\text{ft})/\overline{\Delta T}_C\right]\left[(5119.5\text{ BTU/hr})t - (9.6\text{ BTU/hr-}^0\text{F})\right.$$
$$\left.\Delta T_{A_T} - (2.3\text{ BTU/hr-}^0\text{F})\ \Delta T_{A_P}\right]$$

Subscript denotes temperature.

$$k_{H_{203}} = \left[(.005/\text{ft})/(3.65^0\text{F})\right]\left[(5119.5\text{ BTU/hr})(5/38)\right.$$
$$- (9.6\text{ BTU/hr-}^0\text{F})28.7^0\text{F}) - (2.3\text{ BTU/hr-}^0\text{F})$$
$$\left.(16.6^0\text{F})\right]$$

$$k_{H_{203}} = .49\text{ BTU/hr-ft-}^0\text{F}$$

$$k_{H_{193}} = \left[(.005/\text{ft})/3.25^0\text{F})\right]\left[(5119.5\text{ BTU/hr})(5/38)\right.$$
$$- (9.6\text{ BTU/hr-}^0\text{F})(25.8^0\text{F}) - (2.3\text{ BTU/hr-}^0\text{F})$$
$$\left.(17.2^0\text{F})\right]$$

$$k_{H_{193}} = .57 \text{ BTU/hr-ft-}^0\text{F}$$

$$k_{H_{141}} = \left[(.005/\text{ft})/(1.6^0\text{F})\right]\left[(5119.5 \text{ BTU/hr})(5/79) - (9.6 \text{ BTU/hr-}^0\text{F})(15.4^0\text{F}) - (2.3 \text{ BTU/hr-}^0\text{F})(8.3^0\text{F})\right]$$

$$k_{H_{141}} = .49 \text{ BTU/hr-ft-}^0\text{F}$$

Average thermal conductivity:

$$\bar{k}_H = \left(k_{H_{203}} + k_{H_{193}} + k_{H_{141}}\right)/3 = (.49 + .57 + .49) \text{ BTU/hr-ft-}^0\text{F}/3$$

$$\bar{k}_H = .52 \text{ BTU/hr-ft-}^0\text{F}$$

LIST OF SYMBOLS

Letter Symbols

A	area, $in.^2$
$\bar{A}$	logarithmic mean area, $in.^2$
D	diameter, in.
h	height, in.
I	interference, in.
k	thermal conductivity, BTU/hr-ft-^{0}F
ΔL	oscillograph deflection indicating amount of expansion or thickness, in.
P	power, watts
Q	quantity of heat, BTU
Δr	radial thickness, in.
T	temperature, ^{0}F
ΔT	temperature difference, ^{0}F
t	duty cycle time, sec/sec

Greek Symbols

α	coefficient of linear thermal expansion, in./in.-^{0}F
Δ	oscillograph deflection representing temperature difference, in.

Subscript Symbols

A	asbestos
B	bottom
F	forward bore
H	housing
I	input bore

LIST OF SYMBOLS (CONT'D)

i	inside
L	liner
o	outside
T	tungsten, top, or total